ЖЭТФ/JETP, 2027, том 171, вып. 1, стр. 86–115 © 2027

DYNAMIC PSEUDOGAP MODEL

E. Z. Kuchinskii, M. V. Sadovskii*

Institute for Electrophysics of the Ural Branch of the Russian Academy of Sciences
620016, Ekaterinburg, Russia

Received August 20, 2026,
revised version October 07, 2026
Accepted for publication November 13, 2026

We formulate a theory of pseudogap formation generated by dynamic finite nesting vector $\mathbf{Q}$ fluctuations with characteristic oscillation frequency ω_0, and damping γ. Starting from a Hamiltonian describing electrons coupled to a classical Gaussian random field, we introduce the double-series representations of the single-particle Green's function within an Abelian (commuting) approximation to the exact SU(2) time evolution of the pseudogap problem. The resulting propagator naturally acquires a generalized Bogoliubov structure in which every stochastic scattering history is characterized by an effective dynamic gap, leading to a coherent superposition of dynamically broadened sidebands with complex Poisson weights. A central result of the theory is the emergence of a dynamically generated decoherence scale Γ_{eff} governing the crossover between two qualitatively different pseudogap regimes. For $\omega_0 > \Gamma_{\text{eff}}$ the fluctuating field is resolved coherently and the double-series representation provides a controlled description of dynamic sideband formation. Conversely, when $\Gamma_{\text{eff}} \gtrsim \omega_0$, coherence is progressively lost and the theory crosses over to the quasistatic fluctuating-gap regime described by the exact continued-fraction solution. The coherent and quasistatic descriptions are therefore interpreted as two complementary asymptotic limits of the same microscopic dynamic pseudogap model. The detailed results of numerical calculations for electron spectral density and density of states supporting our approach are presented for different sets of model parameters confirming the general picture of this crossover.

Keywords: pseudogap, dynamic fluctuations of short-range order, charge-density waves, Keldysh model, Green's function, spectral density

DOI: 10.31857/S0044451027010077

1. INTRODUCTION

The properties of electrons in metals interacting with strong short-range order fluctuations have attracted continuous interest for several decades. Examples include charge-density-wave (CDW), spin-density-wave (SDW) and excitonic fluctuations, fluctuating Peierls order [1], as well as the pseudogap phenomena observed in underdoped cuprate superconductors [2–4].

A number of exactly (or nearly exactly) solvable models for one-dimensional electrons interacting with pseudogap were developed based on the complete diagrammatic series generated by the static Gaussian random field, which can be summed exactly in the form of continued-fraction recursion relations. These solutions constitute the basis of the fluctuating-gap model and provide a remarkably accurate description of pseudogap formation in systems with finite correlation length [5–10].

These models were later generalized to two-dimensional case with special emphasis on pseudogap physics in cuprates and other strongly correlated systems [11–18].

The static theory, however, neglects the intrinsic dynamics of the fluctuating order parameter. Near structural or electronic phase transitions the characteristic fluctuation frequency may become comparable to electronic energy scales, making temporal fluctuations an essential part of the problem. A systematic extension of the fluctuating-gap formalism to finite temporal correlation time therefore represents an important open problem.

Recently we obtained [19] an exact solution for electrons interacting with a spatially uniform ($Q = 0$) Gaussian random field with finite temporal correlations, generalizing the earlier dynamic reformulation

* E-mail: sadovski@iep.uran.ru

of exactly solvable Keldysh model [5] introduced by Kikoin and Kiselev [20, 21]. Using generalized Ward identities we derived exact recursion relations for the Green's function and demonstrated that the solution admits an explicit double-series representation describing coherent dynamic sidebands.

The present work addresses the considerably more complicated problem of dynamic pseudogap fluctuations with a finite scattering vector $\mathbf{Q}$. Unlike the $Q = 0$ case, every scattering event transfers an electron between the nested regions of the Fermi surface, producing an alternating sequence of propagators with dispersions $\xi_{\mathbf{k}}$ and $\xi_{\mathbf{k}+\mathbf{Q}}$, giving rise to an effective SU(2) pseudospin structure absent in the uniform problem.

Our primary goal is to construct an analytical description of this dynamic finite-Q problem within the physically important regime where the fluctuating order parameter may be regarded as a classical Gaussian random field with finite temporal correlation time. Employing an exact cumulant resummation of the commuting (Abelian) part of the time-evolution operator, we derive explicit double-series Green's functions for both commensurate and incommensurate fluctuations.

A central result of the present work is that every dynamic scattering history may be associated with an effective complex gap parameter. This naturally leads to a generalized Bogoliubov representation in which the full Green's function is expressed as a coherent superposition of dynamically broadened quasiparticle branches of Bogoliubov quasiparticles, producing spectral densities with dynamically generated sidebands and densities of states with dynamically induced modulation.

The coherent dynamic theory is shown to possess a well-defined domain of applicability controlled by the competition between the characteristic oscillation frequency of the fluctuating field and the dynamically generated decoherence rate. When coherent sidebands overlap strongly, the double-series expansion gradually loses convergence and the calculated spectra evolve toward those described by static continued fractions. The static fluctuating-gap theory may be interpreted as the decohered infrared limit of the more general dynamic theory developed here.

2. MICROSCOPIC MODEL

We consider electrons interacting with a fluctuating order parameter characterized by a finite ordering wave vector $\mathbf{Q}$. Such a model describes electronic scattering from short-range CDW, SDW, excitonic, or Peierls fluctuations. Throughout the present work the fluctuating field is assumed to be classical, while the electronic subsystem is treated fully quantum mechanically.

The electronic Hamiltonian is written as

$$H(t) = H_0 + H_{\rm int}(t), \tag{1}$$

where

$$H_0 = \sum_{\mathbf{k}} \xi_{\mathbf{k}} c^\dagger_{\mathbf{k}} c_{\mathbf{k}} \tag{2}$$

describes noninteracting electrons measured relative to the chemical potential.

The interaction with the fluctuating order parameter is

$$H_{\rm int}(t) = \sum_{\mathbf{k}} \left[\Delta(t) c^\dagger_{\mathbf{k}+\mathbf{Q}} c_{\mathbf{k}} + \Delta^*(t) c^\dagger_{\mathbf{k}} c_{\mathbf{k}+\mathbf{Q}} \right], \tag{3}$$

where $\Delta(t)$ denotes a spatially uniform but temporally fluctuating complex random field.

Equation (3) describes repeated scattering between two nested regions of the Fermi surface separated by the ordering vector $\mathbf{Q}$. Every interaction event transfers an electron according to $\mathbf{k} \longleftrightarrow \mathbf{k} + \mathbf{Q}$, which constitutes the essential difference between the present problem and the previously studied $Q = 0$ dynamic model.

In most part of the paper we consider one-dimensional (Peierls-like CDW) system, though generalization for two-dimensional case (scattering between hot-spots on two-dimensional Fermi surface) in principle is straightforward [4, 11–13].

An alternative schematic derivation of our approach based on Keldysh technique is presented in Appendix A.

2.1. Commensurate and Incommensurate Fluctuations

The physical nature of the fluctuating field (order parameter) depends on the symmetry of the underlying ordered state.

For commensurate ordering one may choose the order parameter to be real,

$$\Delta(\mathbf{r}, t) = 2\Delta(t) \cos(\mathbf{Q} \cdot \mathbf{r}), \tag{4}$$

so that $\Delta(t) = \Delta^*(t)$.

For incommensurate order the order parameter is complex,

$$\Delta(\mathbf{r}, t) = \Delta(t) e^{i\mathbf{Q}\cdot\mathbf{r}} + \Delta^*(t) e^{-i\mathbf{Q}\cdot\mathbf{r}} = \\ = 2\Delta \cos(\mathbf{Q} \cdot \mathbf{r} + \phi), \tag{5}$$

where the complex amplitudes describe independent fluctuations of the two components of the order parameter, Δ and ϕ are the modulus and the phase of the order parameter, both random.

The distinction between these two cases becomes essential in the dynamic problem because the individual scattering histories acquire different effective gap parameters, leading to different structure of Green's functions.

More details on commensurate and incommensurate fluctuations are discussed in Appendix B.

2.2. Gaussian Statistics

The fluctuating field is assumed to obey Gaussian statistics with zero average,

$$\langle \Delta(t) \rangle = 0, \tag{6}$$

and correlation function

$$\langle \Delta(t)\Delta^*(0) \rangle = \Delta^2 e^{-\gamma|t|}\cos(\omega_0 t). \tag{7}$$

Here

- Δ determines the characteristic fluctuation amplitude,
- γ^{-1} is the temporal correlation time,
- ω_0 denotes the characteristic oscillation frequency of the dynamic order parameter.

Equation (7) represents the simplest stationary random process supplemented by coherent oscillations. The exponential form is particularly convenient because repeated time integrations generated by the diagrammatic expansion may be evaluated analytically.

For incommensurate order one additionally has

$$\langle \Delta(t)\Delta(0) \rangle = 0, \qquad \langle \Delta^*(t)\Delta^*(0) \rangle = 0, \tag{8}$$

whereas for commensurate fluctuations the field is real and only a single independent correlator remains.

2.3. Nambu Representation

Throughout most of this paper we consider the vicinity of a nested part (hot-spots) of the Fermi surface satisfying $\xi_{\mathbf{k}+\mathbf{Q}} \simeq -\xi_{\mathbf{k}} \equiv -\xi$, so that every scattering event changes the sign of the electronic dispersion $\xi \longrightarrow -\xi \longrightarrow \xi \longrightarrow \cdots$, which will simplify the subsequent analysis. For incommensurate fluctuations we neglect the states with $\mathbf{k} \pm 2\mathbf{Q}$ and higher momentum transfers and use the two-patch linearized ($Q \approx 2p_F$) approximation. Unlike the uniform ($Q = 0$) [19] problem, successive scattering events therefore alternate between two branches of the electronic spectrum. This alternating structure is ultimately responsible for the generalized Bogoliubov – Gor'kov form of the dynamic Green's function derived below.

It is convenient to introduce the two-component Nambu spinor [22]

$$\hat{\Psi}_{\mathbf{k}} = \begin{pmatrix} c_{\mathbf{k}} \\ c_{\mathbf{k}+\mathbf{Q}} \end{pmatrix}, \tag{9}$$

in terms of which Eq. (1) assumes the compact form

$$H(t) = \sum_{\mathbf{k}} \hat{\Psi}^{\dagger}_{\mathbf{k}} \hat{H}(t) \hat{\Psi}_{\mathbf{k}}, \tag{10}$$

with

$$\hat{H}(t) = \xi\sigma_3 + \Delta(t)\sigma_+ + \Delta^*(t)\sigma_-, \tag{11}$$

where

$$\sigma_{\pm} = \frac{1}{2}(\sigma_1 \pm i\sigma_2) \tag{12}$$

are the standard pseudospin raising and lowering operators.

For a commensurate order parameter Eq. (11) reduces to

$$\hat{H}(t) = \xi\sigma_3 + \Delta(t)\sigma_1, \tag{13}$$

whereas for incommensurate fluctuations both σ_+ and σ_- components (fluctuations) remain independent.

The finite-Q problem therefore possesses an intrinsic SU(2) pseudospin structure originating entirely from the repeated alternation between the nested electronic branches. This noncommutative structure will be shown to generate the certain Magnus corrections absent in $Q = 0$ model.

2.4. Exact Time Evolution and SU(2) Structure

The retarded Green's function of a quantum particle interacting with dynamic external field is defined by an equation:

$$\left(i\frac{\partial}{\partial t} - \hat{H}(t)\right)\hat{G}^R(t,t') = \delta(t-t'). \tag{14}$$

Its solution is

$$\hat{G}^R(t,t') = -i\theta(t-t')U(t,t'), \tag{15}$$

where time-evolution operator is given by

$$U(t,t') = T\exp\left[-i\int_{t'}^{t}\hat{H}(\tau)d\tau\right], \tag{16}$$

where T denotes chronological ordering. In case of the Gaussian random external field $\Delta(t)$ we introduce

$$\hat{G}^R(t) = -i\theta(t)\left\langle T\exp\left[-i\int_0^t dt'\hat{H}(t')\right]\right\rangle_{\Delta}, \tag{17}$$

where we perform the averaging over this random field taking into account Eq. (7).

Equation (17) is formally exact. The principal difficulty of the dynamic finite-Q problem originates from the noncommutativity of the Hamiltonian at different times,

$$[\hat{H}(t_1), \hat{H}(t_2)] \neq 0, \tag{18}$$

which prevents a direct evaluation of the time-ordered exponential.

Using Eq. (11) after straightforward algebra one immediately obtains

$$\begin{aligned}[\hat{H}(t_1), \hat{H}(t_2)] = 2\xi\,[\Delta(t_2) - \Delta(t_1)]\,\sigma_+ - \\ - 2\xi\,[\Delta^*(t_2) - \Delta^*(t_1)]\,\sigma_- + \\ + [\Delta(t_1)\Delta^*(t_2) - \Delta(t_2)\Delta^*(t_1)]\,\sigma_3.\end{aligned} \tag{19}$$

Equation (19) demonstrates that the noncommutativity does not originate from quantum fluctuations of the order parameter. The fluctuating field is purely classical. Instead, it reflects the non-Abelian SU(2) pseudospin algebra associated with repeated scattering between the two nested electronic branches. The commutator vanishes identically only in special limiting cases.

The problem arising here is very similar to the well known difficulties in construction diagrammatic perturbation theory for spin-dependent Hamiltonians in the theory of magnetism. Noncommutativity of spin operators requires the reformulation of the standard Wick theorem and leads to rather complicated variants of diagram technique as proposed in Refs. [23–27]. Below we follow rather simplified approach neglecting pseudospin structure of the vertices in our theory.

2.5. Commuting (Abelian) Limit

The simplest case corresponds to an electron at the Fermi surface, $\xi = 0$. For commensurate (real order parameter $\Delta(t)$) fluctuations,

$$\Delta(t) = \Delta^*(t), \tag{20}$$

the Hamiltonian becomes

$$\hat{H}(t) = \Delta(t)\sigma_1, \tag{21}$$

so that

$$[\hat{H}(t_1), \hat{H}(t_2)] = 0. \tag{22}$$

Chronological ordering therefore becomes unnecessary,

$$T\exp\left[-i\int_0^t dt'\hat{H}(t')\right] = \exp\left[-i\int_0^t dt'\hat{H}(t')\right]. \tag{23}$$

Consequently the dynamic problem reduces to the evaluation of an ordinary Gaussian average and admits an exact cumulant resummation. This observation forms the basis of the double-series representation derived below.

For incommensurate fluctuations (complex order parameter Δ) it is not so in general as is clearly seen from (19) as commutator remains finite even at $\xi = 0$.

Away from the Fermi surface in commensurate case $\xi \neq 0$, and for incommensurate case in general, the Hamiltonians at different times no longer commute.

The evolution operator may formally be written in the Magnus form [28]:

$$U(t) = \exp\left[\Omega_1 + \Omega_2 + \Omega_3 + \cdots\right], \tag{24}$$

where

$$\Omega_1 = -i\int_0^t dt'\hat{H}(t'), \tag{25}$$

while the leading correction is

$$\Omega_2 = -\frac{1}{2}\int_0^t dt_1 \int_0^{t_1} dt_2[\hat{H}(t_1), \hat{H}(t_2)]. \tag{26}$$

The higher Magnus terms describe successive SU(2) rotations of the electronic pseudospin generated by the alternating sequence of finite-Q scattering events.

The finite-Q problem therefore separates naturally into two conceptually distinct ingredients.

The first is the Gaussian stochastic dynamics of the classical order parameter, completely determined by the correlation function (7).

The second is the noncommutative SU(2) evolution of the electronic pseudospin induced by repeated transitions between the nested branches of the Fermi surface. Only the latter is responsible for the Magnus corrections.

Throughout most of the present work we analyze the commuting sector. Actually our numerical calculations show that for a wide and interesting region of the parameters of our model we can identify the parameter region in which the coherent double-series solution provides a reasonable description of dynamic pseudogap physics, while outside this region we can successfully apply another (continued fraction) approximation.

More details on physics of Magnus series effects can be found in Appendix C.

3. EXACT CUMULANT SOLUTION IN THE COMMUTING LIMIT

As discussed in the previous section, the full finite-Q problem is generally non-Abelian owing to the non-commutativity of the Hamiltonian at different times. However, in special case of electron on the Fermi surface for commensurate fluctuations, the Hamiltonians commute and the time-ordered exponential in Eq. (17) simplifies considerably.

Actually the same approximation becomes exact also for the case of generalized Keldysh model, corresponding to $Q = 0$ [19].

In general case we shall consider commuting approximation as a reasonable first step also in general case and try to determine its region of applicability, when the simple cumulant expansion provides accurate enough description of our model.

3.1. Time-Domain Green's Function

Consider first the $Q = 0$ problem with real $\Delta(t)$ when the retarded Green's function becomes

$$G^R(t) = -i\theta(t)e^{-i\xi t}\left\langle \exp\left[-i\int\limits_0^t dt'\Delta(t')\right]\right\rangle. \quad (27)$$

Since the fluctuating field obeys Gaussian statistics, all cumulants higher than second order vanish identically. The Gaussian average is therefore evaluated exactly by the standard cumulant theorem [29],

$$\left\langle e^A\right\rangle = \exp\left(\frac{1}{2}\left\langle A^2\right\rangle\right), \quad (28)$$

with

$$A = -i\int\limits_0^t dt'\Delta(t'). \quad (29)$$

Consequently

$$G^R(t) = -i\theta(t)e^{-i\xi t}e^{-K(t)}, \quad (30)$$

where the cumulant function is

$$K(t) = \frac{1}{2}\int\limits_0^t dt_1\int\limits_0^t dt_2\,\langle\Delta(t_1)\Delta(t_2)\rangle. \quad (31)$$

Equation (30) constitutes the Green's function within the commuting approximation, which is actually exact in the $Q = 0$ problem.

3.2. Evaluation of the Cumulant and Emergent Dynamic Decoherence

Using the exponential representation of our correlation function

$$\langle\Delta(t)\Delta(0)\rangle = \frac{1}{2}\Delta^2 e^{-\gamma|t|}[e^{-i\omega_0 t} + e^{i\omega_0 t}], \quad (32)$$

the double time integration in (31) may be performed analytically, as shown below.

An important consequence of the cumulant representation is the natural emergence of an effective dynamic decoherence rate governing the long-time behavior of the electronic propagator. Considering for shortness only the first term in (32) and introducing $u = t_1 - t_2$, one can write (31) as convolution

$$K(t) = \int\limits_0^t du(t-u)D(u), \quad (33)$$

where

$$D(u) = \frac{1}{2}\Delta^2 e^{-\gamma u}e^{-i\omega_0 u}, \qquad u > 0, \quad (34)$$

and the long-time limit may be analyzed by separating the cumulant into time-independent and time-dependent parts.

Equation (33) may be rewritten as

$$K(t) = t\int\limits_0^t du\,D(u) - \int\limits_0^t du\,uD(u). \quad (35)$$

For times much longer than correlation time, $t \gg \gamma^{-1}$, the upper integration limit may be extended to infinity with exponentially small error,

$$K(t) = Bt - C + O(e^{-\gamma t}), \quad (36)$$

where

$$B = \int\limits_0^\infty du\,D(u), \quad (37)$$

and

$$C = \int\limits_0^\infty du\,uD(u). \quad (38)$$

The coefficient B is readily evaluated,

$$B = \frac{1}{2}\Delta^2\int\limits_0^\infty du\,e^{-(\gamma+i\omega_0)u} = \frac{\Delta^2}{2(\gamma+i\omega_0)}. \quad (39)$$

Separating real and imaginary parts,

$$B = \frac{1}{2}\left[\frac{\gamma\Delta^2}{\omega_0^2+\gamma^2} - i\frac{\omega_0\Delta^2}{\omega_0^2+\gamma^2}\right], \quad (40)$$

one immediately identifies two physically distinct contributions. The imaginary part produces a renormalization (shift) of the quasiparticle energy,

$$\delta\xi = -\frac{1}{2}\frac{\omega_0\Delta^2}{\omega_0^2+\gamma^2}, \tag{41}$$

whereas the real part generates irreversible decay of the propagator. Accordingly we define the effective dynamic decoherence rate

$$\Gamma_{\text{eff}} = \text{Re}\int_0^\infty dt\,\langle\Delta(t)\Delta(0)\rangle = \frac{\gamma\Delta^2}{\omega_0^2+\gamma^2}. \tag{42}$$

The contribution of the first term in (32) to the Green's function therefore assumes the asymptotic form

$$G(t) \sim e^{-i(\xi+\delta\xi)t}e^{-\frac{1}{2}\Gamma_{\text{eff}}t}. \tag{43}$$

Equation (42) demonstrates that Γ_{eff} is not an additional phenomenological broadening parameter but follows directly from the integrated temporal correlations. It measures the irreversible loss of phase coherence caused by repeated scattering from the dynamic pseudogap field. The limiting behavior follows immediately from Eq. (42).

For slowly decaying fluctuations,

$$\gamma \ll \omega_0, \tag{44}$$

one finds

$$\Gamma_{\text{eff}} \simeq \frac{\gamma\Delta^2}{\omega_0^2}, \tag{45}$$

so that decoherence increases linearly with the inverse correlation time.

In the opposite motional narrowing limit,

$$\gamma \gg \omega_0, \tag{46}$$

the decoherence rate becomes

$$\Gamma_{\text{eff}} \simeq \frac{\Delta^2}{\gamma}, \tag{47}$$

which decreases with increasing fluctuation rate. Rapid fluctuations therefore average themselves out before electrons can accumulate a significant scattering phase, restoring coherent quasiparticle motion.

The quantity Γ_{eff} naturally determines the crossover between coherent and incoherent pseudogap dynamics. Indeed, the characteristic electronic coherence time is

$$\tau_\phi = \Gamma_{\text{eff}}^{-1}, \tag{48}$$

whereas the characteristic oscillation period of the fluctuating field is

$$\tau_{\text{osc}} = \omega_0^{-1}. \tag{49}$$

Coherent sidebands remain well resolved provided

$$\tau_\phi \gg \tau_{\text{osc}}, \tag{50}$$

or equivalently,

$$\omega_0 \gg \Gamma_{\text{eff}}. \tag{51}$$

When the opposite inequality holds,

$$\Gamma_{\text{eff}} \gg \omega_0, \tag{52}$$

electrons lose phase memory before resolving the intrinsic oscillations of the fluctuating field. The dynamics then becomes effectively quasistatic, explaining the crossover toward the static fluctuating-gap description discussed in the following sections.

Finally, it is worth emphasizing that the representation (42) is formally identical to the expressions governing decoherence in Kubo stochastic line-shape theory and motional narrowing in magnetic resonance [30].

Now, direct evaluation of the convolution integral with the account of both signs of ω_0 in (32) gives

$$K(t) = \frac{\Delta^2}{2(\gamma+i\omega_0)^2}\left[(\gamma+i\omega_0)t - 1 + e^{-(\gamma+i\omega_0)t}\right] + \\ + \frac{\Delta^2}{2(\gamma-i\omega_0)^2}\left[(\gamma-i\omega_0)t - 1 + e^{-(\gamma-i\omega_0)t}\right]. \tag{53}$$

The first terms inside the square brackets are linear in time

$$Bt = \left[\frac{1}{2}\Gamma_{\text{eff}} \pm i\delta\xi\right]t, \tag{54}$$

and therefore simply generate

$$e^{-K(t)} = e^{-\Gamma_{\text{eff}}t}e^{-K_{\text{ren}}(t)}, \tag{55}$$

where

$$K_{\text{ren}}(t) = \lambda_1\left[1-e^{-\alpha_+t}\right] + \lambda_2\left[1-e^{-\alpha_-t}\right], \tag{56}$$

where we have introduced

$$\alpha_\pm = \gamma \pm i\omega_0, \tag{57}$$

and

$$\lambda_1 = \frac{\Delta^2}{2(\omega_0-i\gamma)^2}, \qquad \lambda_2 = \frac{\Delta^2}{2(-\omega_0-i\gamma)^2}. \tag{58}$$

Equation (56) contains only the bounded oscillatory part of the cumulant. This procedure is entirely analogous to the standard decomposition of a self-energy into an energy shift and damping rate.

3.3. Double-Series Representation of the Dynamic Green's Function

As shown below, the exponential structure of the cumulant naturally generates a double Poisson series, in which every term corresponds to a particular sequence of coherent dynamic scattering events. Substituting (55) and (56) into Eq. (30) we get

$$G^R(t) = -i\theta(t)e^{-i\xi t}e^{-\Gamma_{\text{eff}}t}\times \\ \times \exp(-\lambda_1-\lambda_2)\exp\left[\lambda_1 e^{-\alpha_+ t}+\lambda_2 e^{-\alpha_- t}\right]. \quad (59)$$

Expanding the second exponential here we immediately obtain

$$G^R(t) = -i\theta(t)e^{-i\xi t}e^{-\Gamma_{\text{eff}}t}e^{-\lambda_1-\lambda_2}\times \\ \times \sum_{n,m=0}^{\infty} W_{nm}e^{-(n+m)\gamma t}e^{-i(n-m)\omega_0 t}, \quad (60)$$

where

$$W_{nm} = \frac{\lambda_1^n\lambda_2^m}{n!m!}. \quad (61)$$

The Fourier transform of Eq. (60) is elementary:

$$G^R(\omega) = \int_0^{\infty} dt\, e^{i\omega t}G^R(t), \quad (62)$$

giving

$$G^R(\omega,\xi) = e^{-\lambda_1-\lambda_2}\sum_{n,m=0}^{\infty} W_{nm}\times \\ \times \frac{1}{\omega-\xi-(n-m)\omega_0+i(n+m)\gamma+i\Gamma_{\text{eff}}}, \quad (63)$$

where we have explicitly separated an additional decoherence scattering rate Γ_{eff} whose physical origin was discussed above in Sec. 3.2.

Equation (63) is the exact coherent double-series representation for $Q = 0$ problem (when the commuting approximation is exact). It can be written in convenient equivalent form as

$$G^R(\omega,\xi) = \sum_{n,m=0}^{\infty} P_{\lambda_1}(n)P_{\lambda_2}(m)\times \\ \times \frac{1}{\omega-\xi-(\omega_0-i\gamma)(n-\lambda_1)-(-\omega_0-i\gamma)(m-\lambda_2)}, \quad (64)$$

where we have introduced complex Poisson distributions

$$P_{\lambda_i}(k) = \frac{\lambda_i^k}{k!}\exp(-\lambda_i),\ i = 1,2. \quad (65)$$

Actually, Eqs. (63), (64) represent an exact solution of Keldysh $Q = 0$ model and the procedure described above gives an alternative way to derive this result as compared with diagrammatic approach of Ref. [19].

3.4. Dynamic Scattering Histories and Sidebands

Each pair of integers (n, m) labels one elementary dynamic history. The integer n counts the number of scattering events associated with the positive frequency component $e^{-i\omega_0 t}$, while m counts the corresponding number for the negative-frequency component $e^{+i\omega_0 t}$. Consequently $n - m$ determines the net dynamical energy shift, whereas $n + m$ governs the accumulated decoherence produced by the finite temporal correlation time. The Green's function therefore appears as a coherent superposition of infinitely many dynamically broadened sidebands.

Unlike ordinary Poisson probabilities, our distributions $P_{\lambda_i}(k)$ are in general complex containing both damping and oscillatory contributions. Consequently, the individual histories cannot be interpreted as classical probabilities. Instead, they represent coherent amplitudes that interfere after summation over all dynamic histories. Only the complete Green's function possesses direct physical meaning.

From Eq. (63) it is obvious that dynamic spectrum consists of an infinite family of equidistant sidebands separated by the characteristic fluctuation frequency. The intensity of each sideband is determined by the corresponding complex Poisson amplitude, while its width increases linearly with the total number of scattering events. The resulting structure resembles a Floquet spectrum. However, unlike conventional Floquet systems generated by periodic driving, the present sidebands arise entirely from stochastic Gaussian dynamics and remain intrinsically broadened by the finite correlation time of the fluctuating order parameter.

4. GENERALIZED BOGOLIUBOV REPRESENTATION OF DYNAMIC HISTORIES

4.1. History-Dependent Nambu Gaps

For finite Q problem each scattering event transfers an electron from one side of the Fermi surface to the other, or from one Nambu branch to another one. To generalize our $Q = 0$ treatment to this case we have to define the set of random matrix Poissonian fields which are non-diagonal in Nambu representation. We must stress that our derivation is based on rather heuristic

physical assumptions and is justified mostly by the results of our detailed numerical calculations presented below, which demonstrate the full agreement with the known exactly solvable limits of the model under discussion. The rigorous derivation requires further studies, which we leave for the future.

For commensurate fluctuations, starting from the obvious analogy with exactly solvable $Q = 0$ model, we introduce two matrix dynamic scattering fields as

$$\begin{aligned}\hat{\Delta}_{1n} &= \sigma_1\Delta_{1n} = \sigma_1(\omega_0 - i\gamma)(n - \lambda_1),\\ \hat{\Delta}_{2m} &= \sigma_1\Delta_{2m} = \sigma_1(-\omega_0 - i\gamma)(m - \lambda_2),\end{aligned} \tag{66}$$

distributed according to complex Poisson distributions defined in (65). The corresponding complex pseudogap scale is

$$\Delta_{nm} = \Delta_{1n} + \Delta_{2m}, \tag{67}$$

so that the acting Poissonian field is

$$\begin{aligned}\hat{\Delta}_{nm} = \sigma_1\Delta_{nm} = \sigma_1(\omega_0 - i\gamma)(n - \lambda_1)+\\ + \sigma_1(-\omega_0 - i\gamma)(m - \lambda_2).\end{aligned} \tag{68}$$

Note that

$$\Delta_{nm} = (n - m)\omega_0 - i(n + m)\gamma - i\Gamma_{\text{eff}}, \tag{69}$$

where we explicitly separated $i\Gamma_{\text{eff}}$ contribution from (68) where it is somehow hidden. The sign of this imaginary quantity here is convention-dependent because it depends on the Fourier and retarded Green's function conventions.

Now for a given history (n, m) the effective Nambu matrix Hamiltonian is assumed to take the following form:

$$\hat{H}_{nm} = \xi\sigma_3 + \Delta_{nm}\sigma_1, \tag{70}$$

so that Δ_{nm} generates non-diagonal scattering in Nambu space producing gaps.

The corresponding (n, m) history Green's function for finite ξ is written as

$$\hat{G}_{nm}(\omega, \xi) = [(\omega + i\Gamma_{\text{eff}})\sigma_0 - \xi\sigma_3 - \Delta_{nm}\sigma_1]^{-1}, \tag{71}$$

where we have explicitly added the effective damping introducing the substitution $\omega \to \omega + i\Gamma_{\text{eff}}$ in the diagonal part of the history Green's function. This is necessary to suppress unphysical contributions from $n = m$ terms, reflected in the appearance of pathological discrete poles with both positive and negative weights contributions to spectral density. The precise value of this damping equal to Γ_{eff} is actually the minimal one sufficient to suppress these unphysical singularities. This was explicitly checked by our numerical calculations.

Our numerical calculations also show that this substitution also ensures the full agreement with the results obtained for $\omega_0 = 0$ case from the exact continued fraction representation to be discussed below in the limit of large γ. However, this substitution leads to inevitable double-counting of effective damping Γ_{eff} in case of $\xi = 0$, where we actually have an exact solution, the same as in Keldysh model [19]. To avoid this double counting in numerical calculations we have to redefine Δ_{nm} in commensurate case by subtracting Γ_{eff}: $\Delta_{nm} \to (n-m)\omega_0 - i(n+m)\gamma$. We have explicitly checked numerically that such subtraction guarantees the reproducibility of an exact solution of our model at $\xi = 0$. We must stress that this is to be done only in the diagonal part of $\hat{G}_{nm}$ to avoid double counting problem and restore the exact solution for $\xi = 0$. The physical definition of the dynamic gap Δ_{nm} remains that of Eq. (68), which in particular guarantees the absence of average anomalous Green's function in our problem (see below Eq. (101)).

Finally we obtain the Nambu matrix representation of the single (n, m) history Green's function as

$$\hat{G}_{nm}(\omega, \xi) = \frac{(\omega + i\Gamma_{\text{eff}})\sigma_0 + \xi\sigma_3 + \Delta_{nm}\sigma_1}{(\omega + i\Gamma_{\text{eff}})^2 - \xi^2 - \Delta_{nm}^2}. \tag{72}$$

The complex quasiparticle energy is defined as

$$E_{nm} = \sqrt{\xi^2 + \Delta_{nm}^2}. \tag{73}$$

The square root here must be assigned the retarded branch. In the numerical implementation, this is implemented by first evaluating the principal complex square root and then imposing

$$\operatorname{Im} E_{nm} \le 0, \tag{74}$$

and

$$E_{nm} \to -E_{nm} \qquad \text{if} \qquad \operatorname{Im} E_{nm} > 0. \tag{75}$$

This branch prescription is essential for maintaining the retarded analytic structure of each history.

4.2. Bogoliubov Decomposition

The Nambu expression for the Green's function can alternatively be decomposed into Bogoliubov form. We define Bogoliubov coefficients as

$$u_{nm}^2 = \frac{1}{2}\left(1 + \frac{\xi}{E_{nm}}\right), \tag{76}$$

and

$$v_{nm}^2 = \frac{1}{2}\left(1 - \frac{\xi}{E_{nm}}\right), \tag{77}$$

which satisfy

$$u_{nm}^2 + v_{nm}^2 = 1. \quad (78)$$

The component of the retarded propagator associated with one history is then represented as

$$G_{nm}^R(\omega,\xi) = \frac{u_{nm}^2}{\omega + i\Gamma_{\text{eff}} - E_{nm}} + \\ + \frac{(v_{nm}^2)^*}{\omega + i\Gamma_{\text{eff}} + E_{nm}^*}. \quad (79)$$

Combining the Poisson histories with the Nambu matrix gives the history averaged Green's function:

$$G^R(\omega,\xi) = e^{-\lambda_1-\lambda_2}\sum_{n,m}\left[W_{nm}\frac{u_{nm}^2}{\omega + i\Gamma_{\text{eff}} - E_{nm}} + \right. \\ \left. + W_{nm}^*\frac{(v_{nm}^2)^*}{\omega + i\Gamma_{\text{eff}} + E_{nm}^*}\right]. \quad (80)$$

The first term here represents propagation through the positive-energy Nambu branch, whereas the second is the conjugated negative-energy branch. The conjugation of both the Poisson weight and the coherence factor is required to reproduce the retarded Green's function structure.

In the following for shortness we use the following notation:

$$\tilde{\omega} = \omega \pm i\Gamma_{\text{eff}}, \quad (81)$$

to fix the retarded or advanced behavior of the Green's function.

4.3. Central Result for the Green's Function

Thus the double-series representation admits a clear formulation for our finite Q problem. Instead of interpreting every term as an independent dynamic sideband, each scattering history may be regarded as an effective Bogoliubov quasiparticle characterized by a complex dynamic gap parameter. Near a nested portion of the Fermi surface the electronic states $\mathbf{k}$ and $\mathbf{k} \pm \mathbf{Q}$ become strongly mixed by the fluctuating density-wave order parameter. We use Nambu notations (9)–(11) and work with corresponding matrix Green's functions.

The essential complication of the dynamic finite-Q problem is not the Gaussian averaging itself but the noncommutativity of the SU(2) matrices appearing at different scattering vertices. The central approximation adopted in the present work consists in projecting this ordered SU(2) algebra onto its commuting (Abelian) sector.

We associate with every stochastic history (n,m) an effective Bogoliubov Hamiltonian (70). The corresponding history Green's function is defined by $(1,1)$ matrix element of the Nambu matrix (72):

$$G_{nm}(\omega,\xi) = \frac{\tilde{\omega} + \xi}{\tilde{\omega}^2 - \xi^2 - \Delta_{nm}^2}, \quad (82)$$

which has exactly the Gor'kov – Bogoliubov form [5,31]. It can be easily seen that for $\xi = 0$ Eq. (82) reduces to the half-sum of two contributions, similar to those entering the (n,m)-sum in Eq. (64) corresponding to $Q = 0$ problem and differing only by the signs of Δ_{nm}.

Equation (82) constitutes the main working approximation of the present theory. It is exact in the commuting limit ($\xi = 0$ for commensurate fluctuations), reproduces the exact static Bogoliubov propagator when $\omega_0 \to 0$ and $\gamma \to 0$, and retains the correct free-electron limit $|\xi| \to \infty$. Away from the commuting limit, deviations originate entirely from the non-Abelian SU(2) vertex algebra neglected in the Abelian projection and will be analyzed later using the Magnus expansion. Actually this is the main approximation of the present work.

The excitation spectrum corresponding to one history is determined by $E_{nm} = \sqrt{\xi^2 + \Delta_{nm}^2}$. Because Δ_{nm} is generally complex, the quasiparticle energy also becomes complex, with the imaginary part describing the finite lifetime generated by the dynamic fluctuations.

Thus every history represents a dynamically broadened Bogoliubov quasiparticle rather than a stationary excitation and the full Green's function is written as history averaged Gor'kov's function:

$$G(\omega,\xi) = \sum_{n,m=0}^{\infty} P_{\lambda_1}(n)P_{\lambda_2}(m)\frac{\tilde{\omega} + \xi}{\tilde{\omega}^2 - \xi^2 - \Delta_{nm}^2}. \quad (83)$$

However, we have to be cautious here to guarantee correct analytical properties. For accurate representation of retarded Green's function we have to use Bogoliubov – Gor'kov form:

$$G^R(\omega,\xi) = \\ = \sum_{n,m=0}^{\infty} P_{\lambda_1}(n)P_{\lambda_2}(m)\frac{u_{nm}^2}{\omega + i\Gamma_{\text{eff}} - \sqrt{\xi^2 + \Delta_{nm}^2}} + \\ + \sum_{n,m=0}^{\infty} P_{\lambda_1}^*(n)P_{\lambda_2}^*(m)\frac{(v_{nm}^2)^*}{\omega + i\Gamma_{\text{eff}} + \sqrt{\xi^2 + (\Delta_{nm}^2)^*}}. \quad (84)$$

Since E_{nm} is complex, the coherence factors (Bogoliubov $u-v$ coefficients) themselves become complex am-

plitudes. They therefore cannot be interpreted as occupation probabilities. Instead they determine the relative weights of electron-like and hole-like components within each coherent scattering history. The complete Green's function is obtained by coherent summation over all histories. Equations (83) and (84) constitute the central analytical result of the present work.

Unlike the conventional Bogoliubov theory, which contains only a single gap parameter, the present dynamic problem generates an infinite family of history-dependent complex gaps. The physical Green's function emerges only after coherent summation over all such histories. The representation (84) admits a simple physical interpretation. The fluctuating order parameter generates an ensemble of dynamically evolving pseudogaps rather than a single static gap. Every coherent history experiences its own effective complex gap (68), determined by the accumulated oscillatory phase and decoherence acquired during the sequence of scattering events. The observed quasiparticle spectrum therefore corresponds not to one Bogoliubov branch but to the coherent superposition of infinitely many dynamic Bogoliubov quasiparticles. This viewpoint provides a natural bridge between the static fluctuating-gap model and the coherent double-series representation developed in the present work. Several important observations follow immediately.

First, the generalized Bogoliubov representation is exact within the commuting approximation and introduces no additional assumptions beyond the double-series expansion itself.

Second, the effective gap (68) is not an externally imposed order parameter but an emergent quantity associated with a particular dynamic scattering history.

The generalized Bogoliubov representation developed up to now naturally describes commensurate pseudogap fluctuations, for which the order parameter is real. For incommensurate fluctuations the situation is qualitatively different. In this case the fluctuating order parameter possesses two independent fluctuating components and the corresponding history Green's functions acquire a different structure.

4.4. Incommensurate Fluctuations

For incommensurate fluctuations the order parameter is intrinsically complex,

$$\Delta(t) = \Delta_1(t) + i\Delta_2(t), \tag{85}$$

where the two real components fluctuate independently. The corresponding Nambu Hamiltonian is

$$\hat{H}(t) = \xi\sigma_3 + \Delta_1(t)\sigma_1 + \Delta_2(t)\sigma_2. \tag{86}$$

The square of this Hamiltonian is given by

$$H^2 = \xi^2 + \Delta_1^2 + \Delta_2^2, \tag{87}$$

so that the spectrum depends only upon the rotationally invariant combination

$$\Delta^2 = \Delta_1^2 + \Delta_2^2. \tag{88}$$

Thus our fluctuating-gap model possesses an internal $O(2)$ symmetry corresponding to rotations in the (Δ_1, Δ_2) plane in Nambu space.

Within the coherent cumulant expansion the Gaussian averages are again performed exactly. Since

$$\langle \Delta(t)\Delta(0)\rangle = 0, \tag{89}$$

while

$$\langle \Delta(t)\Delta^*(0)\rangle \neq 0, \tag{90}$$

the two Cartesian components in Nambu space generate two statistically independent stochastic histories. Accordingly, the commensurate history scalar naturally generalizes to the history vector in two-dimensional pseudospin (Nambu) space

$$\mathbf{\Delta}_{nm} = (\Delta_{1n}, \Delta_{2m}), \tag{91}$$

whose components are introduced as

$$\Delta_{1n} = (\omega_0 - i\gamma)(n - \lambda_1), \tag{92}$$

and

$$\Delta_{2m} = (-\omega_0 - i\gamma)(m - \lambda_2). \tag{93}$$

Now the effective Nambu matrix Hamiltonian for a given history (n, m) is written as

$$\hat{H}_{nm} = \xi\sigma_3 + \Delta_{1n}\sigma_1 + \Delta_{2m}\sigma_2, \tag{94}$$

and corresponding (n, m) history Green's function is given by

$$\hat{G}_{nm}(\omega, \xi) = \\ = [(\omega + i\Gamma_{\text{eff}})\sigma_0 - \xi\sigma_3 - \Delta_{1n}\sigma_1 - \Delta_{2m}\sigma_2]^{-1}. \tag{95}$$

The explicit introduction of effective damping in the denominator here again ensures the numerical agreement with the results of an exact continued fraction solution for the case of $\omega_0 = 0$ and in the limit of large γ. There is no double counting here as Γ_{eff} actually does not enter explicitly our $\Delta_{1n}\sigma_1 - \Delta_{2m}\sigma_2$ combination for incommensurate case.

The effective gap entering the history Green's function must preserve the same $O(2)$ invariant in pseudospin space as in the static theory. We therefore define

$$\mathbf{\Delta}_{nm}^2 = \Delta_{1n}^2 + \Delta_{2m}^2, \tag{96}$$

which represents the natural dynamic generalization of the static gap invariant (88).

Then the (1,1) matrix element of Nambu matrix for corresponding history Green's function is written as

$$G_{nm}(\omega,\xi) = \frac{\tilde{\omega}+\xi}{\tilde{\omega}^2-\xi^2-\mathbf{\Delta}^2_{nm}}. \tag{97}$$

Equation (97) constitutes the minimal $O(2)$-symmetric extension of the commensurate coherent theory. Rather than introducing a single effective complex history gap, each stochastic history is characterized by a two-component history vector whose invariant length determines the quasiparticle spectrum, exactly as in the static fluctuating-gap model.

As in the commensurate theory, the resulting Green's function should be viewed as the central working approximation of the coherent dynamic theory. Its validity is supported by the exact static limit, the correct free-electron limit, and the symmetry of the underlying Nambu Hamiltonian, while corrections originating from the non-Abelian structure of the exact time evolution are expected to appear through the Magnus terms discussed below.

4.5. Unified Physical Picture

The proposed history Green's function possesses the correct static limit for

$$\omega_0 \to 0, \qquad \gamma \to 0. \tag{98}$$

Explicit calculations for this limit are presented in Appendix D. For incommensurate cases we reproduce the familiar result of Refs. [6,7] with Gor'kov's function averaged over Rayleigh distribution of static gaps, while for commensurate case the averaging goes over the usual Gaussian distribution [8].

For finite values of ω_0 the situation changes qualitatively. Every scattering history acquires the energy shift

$$(n-m)\omega_0, \tag{99}$$

together with the damping

$$(n+m)\gamma. \tag{100}$$

The spectrum therefore consists of an infinite family of coherent sidebands, whose amplitudes are determined by the complex Poisson weights.

Average gap is easily shown to be zero

$$\langle\Delta_{nm}\rangle = \sum_{n,m=0}^{\infty} P_{\lambda_1}(n)P_{\lambda_2}(m)\times \\ \times\left[(\omega_0-i\gamma)(n-\lambda_1)+(-\omega_0-i\gamma)(m-\lambda_2)\right]=0, \tag{101}$$

corresponding to the absence of long-range order and vanishing anomalous Green's functions.

The present analysis suggests that the dynamic pseudogap problem possesses three physically distinct regimes.

1. For $\omega_0 \gg \Gamma_{\text{eff}}$, the spectrum is governed by coherent dynamic sidebands described by the double-series representation.

2. For $\omega_0 \sim \Gamma_{\text{eff}}$, the sidebands overlap and coherence is progressively lost. The calculated spectra evolve continuously toward the static ($\omega_0 = 0$) continued-fraction solution.

3. For $\gamma \gg \omega_0, \Delta$, motional narrowing suppresses pseudogap formation altogether and restores conventional free quasiparticle behavior.

The static $\omega_0 = 0$ theory thus appears naturally as quasistatic limit of the more general dynamic theory.

5. EXACT CONTINUED-FRACTION SOLUTION IN THE QUASISTATIC REGIME

As discussed in the previous sections, the coherent double-series representation provides a natural description of the dynamic pseudogap problem whenever the characteristic oscillation frequency of the order parameter exceeds the dynamically generated decoherence scale,

$$\omega_0 > \Gamma_{\text{eff}}. \tag{102}$$

In the opposite regime,

$$\Gamma_{\text{eff}} \gtrsim \omega_0, \tag{103}$$

the electron loses phase coherence before it can resolve the oscillatory motion of the fluctuating field. The dynamics therefore becomes effectively quasistatic, and the finite frequency ω_0 may be neglected in the correlation function. The problem then reduces to a dynamic model with exponentially decaying temporal correlations,

$$\langle\Delta(t)\Delta^*(0)\rangle = \Delta^2 e^{-\gamma|t|}, \tag{104}$$

which admits an exact diagrammatic solution.

It is important to emphasize that this continued-fraction solution should not be regarded as an independent approximation. Rather, it represents the decohered infrared limit of the general dynamic pseudogap problem, complementary to the coherent double-series representation discussed above.

5.1. Exact Diagrammatic Summation

The derivation follows the method originally developed for the one-dimensional static pseudogap problem by one of the present authors [5, 9]. The essential simplification of the present dynamic model is that all internal frequency integrations can be performed exactly by contour integration.

Indeed, every interaction line contributes a Lorentzian frequency dependence possessing only simple poles in the complex frequency plane. As a consequence, every internal frequency integration is evaluated exactly by residues. This should be contrasted with the original static one-dimensional model, where analogous momentum integrations required an asymptotically controlled approximation [13]. In this sense the present dynamic model is exactly solvable.

A remarkable property of the model is that every diagram containing crossing interaction lines is exactly equal to a noncrossing diagram obtained by a suitable relabeling of interaction vertices [5, 9]. Consequently, the complete perturbation series may be generated by considering only rainbow diagrams, provided every interaction line is multiplied by an appropriate combinatorial factor $v(k)$ counting the number of topologically equivalent diagrams.

For commensurate fluctuations,

$$v(k) = k, \tag{105}$$

whereas for incommensurate fluctuations

$$v(k) = \begin{cases} \dfrac{k+1}{2}, & k \text{ odd}, \\ \dfrac{k}{2}, & k \text{ even}. \end{cases} \tag{106}$$

These factors incorporate exactly the contributions of all crossed diagrams.

5.2. Continued-Fraction Recursion

Summation of the complete perturbation series then reduces to the exact recursion relation for the irreducible self-energy,

$$\Sigma_k(\omega,\xi) = \frac{\Delta^2 v(k)}{\omega - (-1)^k\xi + ik\gamma - \Sigma_{k+1}(\omega,\xi)}, \tag{107}$$

which immediately yields the recursion relation for the Green's function,

$$G_k(\omega,\xi) = \big[\omega - (-1)^k\xi + ik\gamma - \\ -\Delta^2 v(k+1) G_{k+1}(\omega,\xi)\big]^{-1}. \tag{108}$$

The physical Green's function is obtained from $G(\omega,\xi) = G_0(\omega,\xi)$. Equivalently, one obtains the exact continued-fraction representation

$$G(\omega,\xi) = \cfrac{1}{\omega - \xi - \cfrac{v(1)\Delta^2}{\omega + \xi + i\gamma - \cfrac{v(2)\Delta^2}{\omega - \xi + 2i\gamma - \cfrac{v(3)\Delta^2}{\omega + \xi + 3i\gamma - \cdots}}}}. \tag{109}$$

Equations (107)–(109) provide the exact solution of the quasistatic dynamic pseudogap model.

5.3. Relation to the Coherent Theory

The present work therefore possesses two complementary nonperturbative descriptions. For

$$\omega_0 > \Gamma_{\text{eff}}, \tag{110}$$

the coherent double-series representation provides a controlled description of dynamically resolved sidebands. Conversely, when

$$\Gamma_{\text{eff}} \gtrsim \omega_0, \tag{111}$$

the continued-fraction solution becomes asymptotically exact because the electron experiences the fluctuating order parameter as effectively quasistatic during its coherence time.

Together, the coherent double-series representation and the exact continued fraction constitute complementary asymptotic descriptions of the same underlying dynamic pseudogap model. As will be demonstrated below, the crossover between the two regimes is accurately controlled by the ratio $\omega_0/\Gamma_{\text{eff}}$.

6. SPECTRAL PROPERTIES OF THE DYNAMIC GREEN'S FUNCTION

The double-series representation obtained above provides an explicit analytical expression for the Green's function. It is therefore important to analyze its fundamental analytical and spectral properties. The electronic spectral density is defined in the usual manner,

$$A(\omega,\xi) = -\frac{1}{\pi}\mathrm{Im}\, G^R(\omega,\xi). \tag{112}$$

The general spectral sum rule is satisfied

$$\int\limits_{-\infty}^{\infty} A(\omega,\xi)\, d\omega = 1, \tag{113}$$

expressing conservation of the total electronic spectral weight. Any numerical implementation of the double-series expansion should satisfy this relation with high accuracy and may therefore use it as a convenient convergence test.

The observable spectrum is obtained as a coherent superposition of the spectral functions associated with individual dynamic histories. For an exact retarded Green's function the spectral density satisfies

$$A(\omega,\xi) \geq 0. \tag{114}$$

However, this positivity property need not hold separately for individual dynamic histories. Indeed, in our case:

- the history weights are generally complex,
- the effective dynamic gaps are complex,
- the generalized Bogoliubov coherence factors also become complex.

Therefore individual terms of the double series should be interpreted as coherent amplitudes rather than independent spectral contributions. Only the complete resummed Green's function is expected to possess a strictly positive spectral density.

6.1. Numerical Results for Spectral Densities and Density of States

We performed extensive numerical calculations of spectral functions of our model (112) using double series representation for the Green's function (83), (84) for dynamic model, making comparison with exact continued fraction solution for the static ($\omega_0 = 0$) case (108). We have explicitly checked that the exact sum rule (113) is satisfied precisely for all values of the parameters of the model used in our calculations.

The double-series representation is especially convenient for numerical calculations and continued fraction algorithm demonstrates very fast convergence. Since the Poisson weights in double series decrease factorially, the sums may be truncated at finite values $n \leq n_{\max}$, $m \leq m_{\max}$, with rapidly controllable accuracy. In our calculations we used the values of $n_{\max}$, $m_{\max}$ with $n_{\max} + m_{\max} \leq 10^3$. The principal numerical limitation is not convergence of the series itself but rather the increasing cancellation between neighboring histories in the strongly overdamped regime. As discussed in the previous section, this behavior signals the crossover from coherent dynamic sidebands toward the quasistatic fluctuating-gap description. Below we show only most typical results obtained for characteristic values of the model parameters.

In Fig. 1 we show spectral densities for the case of commensurate fluctuations with relatively small values of the frequency $\omega_0 = 0.1$ (all energies below are measured in units of the amplitude Δ). First panel shows results at the Fermi surface $\xi = 0$, where our commuting solution is exact. Here we take very small values of damping $\gamma = 0.0001$. The next two panels show spectral density for $\xi \neq 0$, demonstrating typical asymmetric pseudogap behavior. In all these cases we observe characteristic modulation of spectral density with frequency ω_0, around the smooth behavior obtained from exact continued fraction solution for the case of $\omega_0 = 0$ and also shown in these graphs. The last panel of Fig. 1 shows γ dependence of spectral density and corresponding values of Γ_{eff}, demonstrating smooth suppression of sidebands (modulations). Actually these results are very similar to those obtained for spectral density in $Q = 0$ Keldysh model in Ref. [19]. Analogous results for larger $\omega_0 = 0.5$ and $\gamma = 0.02$ are shown in Fig. 2, where at the last panel we again show the γ dependence and suppression of modulations at larger damping.

We have specifically checked that in the limit of large γ our results for $\xi = 0$ smoothly transform to an exact static spectral density calculated from continued fraction solution, confirming the exactness of double-series solution in this case.

In case of the finite ξ, good correlation with continued fraction results is observed only for $\omega_0 \gg \Gamma_{\mathrm{eff}}$. The deviations appearing for large enough γ when $\omega_0 \sim \Gamma_{\mathrm{eff}}$ are attributed to our neglect of the Magnus terms contributions in our commuting approximation. However,

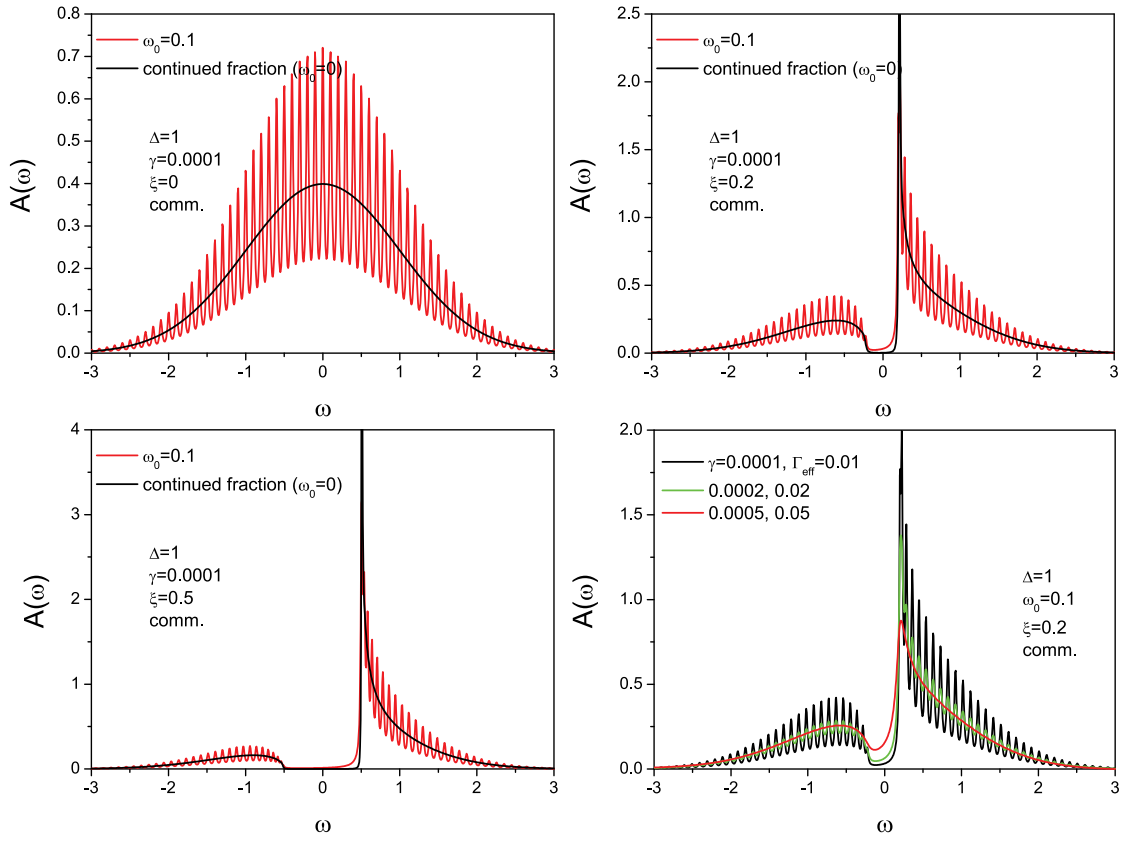

Fig. 1. Spectral density in commensurate case and $\omega_0 = 0.1$ for different values of electron energy ξ. The last panel shows γ dependence of spectral density at $\xi = 0.2$. Black lines on first three panels represent the results for spectral density obtained for static model ($\omega_0 = 0$) from exact continued fractions. All energies are given in units of Δ

it is obvious on physical grounds that for large values of $\Gamma_{\text{eff}} > \omega_0$ the exact static continued fraction solution gives reliable description of spectral density for our dynamic model.

Note that the double-series representation follows from the exact cumulant solution of the commuting sector of the dynamic finite-Q problem. Its validity therefore depends upon the extent to which the neglected non-Abelian SU(2) corrections remain small.

The behavior of spectral densities in case of incommensurate fluctuations is in some sense similar but more complicated. In Fig. 3 we show spectral densities for the case of incommensurate fluctuations for small values of the frequency $\omega_0 = 0.1$. First two panels show results for $\xi = 0$ and $\xi = 0.2$ and very small values of damping $\gamma = 0.0001$. We observe typical pseudogap behavior of spectral density but with seemingly chaotic modulations with frequency ω_0. The next two panels show spectral densities at larger values of $\gamma = 0.02$. Actually in all cases here modulation is regular but peaks at ω_0 harmonics are split due to the existence of two independently fluctuating fields for incommensurate case, which creates more complicated picture of spectral density modulations as compared with commensurate case.

In Fig. 4 we show the γ dependence of spectral density for incommensurate case. In general we observe the suppression of sidebands in the spectral density with growth of γ, similar to commensurate case.

Results obtained from double series are again reliable for $\omega_0 \gg \Gamma_{\text{eff}}$ and continued fraction description is valid for $\Gamma_{\text{eff}} > \omega_0$, with results for this region shown on the last panel of Fig. 4, while the crossover region of $\omega_0 \sim \Gamma_{\text{eff}}$ cannot be reliably described due to the role of neglected Magnus terms. However, it is absolutely clear physically that this crossover is smooth and continuous.

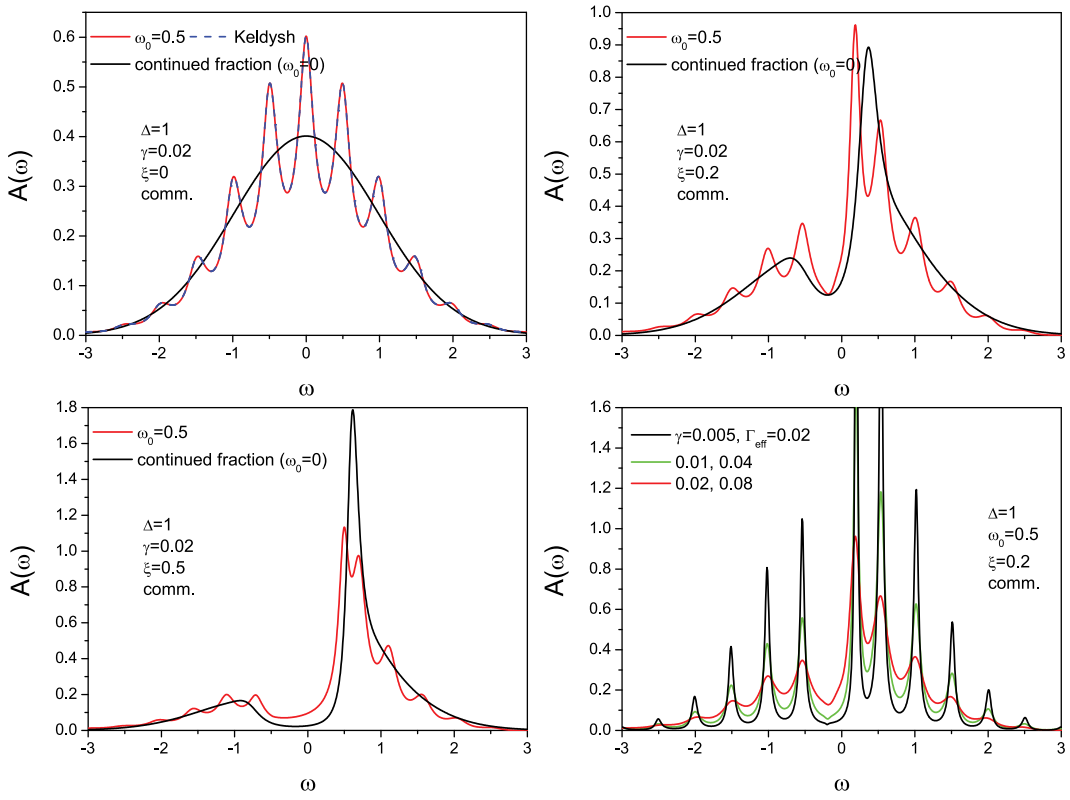

Fig. 2. Spectral density in commensurate case of dynamic pseudogap model with $\omega_0 = 0.5$ for different values of electron energy ξ. Black lines on first three panels represent the exact results for spectral density obtained for static model ($\omega_0 = 0$) from exact continued fractions. The dashed blue line in the first panel represents the exact solution for Keldysh model ($Q = 0$) [19], while the red line shows the exact solution of dynamic pseudogap model for $\xi = 0$. The last panel shows γ dependence of spectral density for fixed $\xi = 0.2$. All energies are given in units of Δ

Total density of states can be directly calculated from its definition:

$$N(\omega) = -\frac{1}{\pi}\int\limits_{-\infty}^{\infty} d\xi \mathrm{Im}\, G^R(\omega,\xi). \qquad (115)$$

For simplicity all calculations were performed for bare electronic band of infinite width. Exact nesting is assumed as usual in one-dimensional case. Both for commensurate and incommensurate fluctuations the density of states demonstrates typical pseudogap behavior with additional peaks due to sidebands (modulation of spectral density with frequency ω_0) as shown in Fig. 5, similar to that observed for Keldysh $Q = 0$ model in Ref. [19]. These peaks are gradually suppressed with the growth of γ as the pseudogap itself which closes at large enough values of γ, as is well known for the case of static fluctuations [9, 10, 13]. This behavior is physically pretty obvious within our approach.

Such additional peaks of the density of states are observable in principle in tunneling experiments.

6.2. General Physical Picture

Thus our numerical results fully confirm the existence of the following three physical regimes in our problem:

6.2.1. Coherent Dynamic Regime

The most favorable situation corresponds to relatively slow decoherence,

$$\omega_0 \gg \Gamma_{\mathrm{eff}}, \qquad (116)$$

where Γ_{eff} denotes the dynamically generated linewidth. In this regime neighboring sidebands remain well resolved, for the dominant scattering histories. The electron therefore retains phase coherence over many oscillation periods of the fluctuating field. The physical spectrum is naturally interpreted as a coherent superposition of dynamically broadened Bogoliubov quasiparticles, and numerical calculations indicate rapid convergence of the double-series expansion.

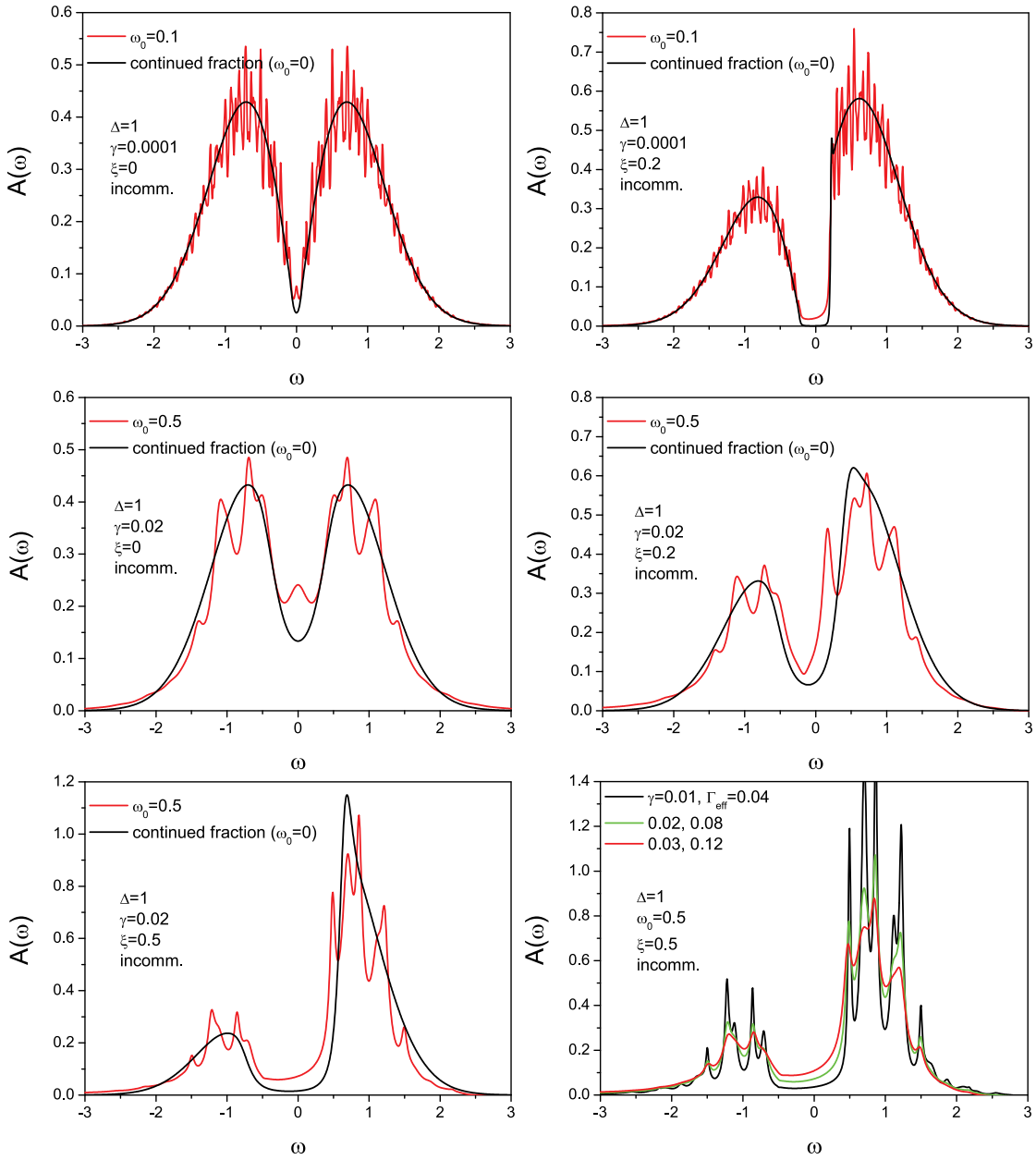

Fig. 3. Spectral density for incommensurate case and $\omega_0 = 0.1, 0.5$ for different values of electron energy ξ. Black lines represent the results for spectral density obtained for static model ($\omega_0 = 0$) from exact continued fractions. Last panel shows dependence of spectral density on γ at $\omega_0 = 0.5$ and $\xi = 0.5$. All energies are given in units of Δ

6.2.2. Crossover Regime

This is the most complicated region where

$$\Gamma_{\text{eff}} \sim \omega_0. \tag{117}$$

Neighboring sidebands begin to overlap and can no longer be regarded as independent coherent excitations. In this region our double series in general overestimates the role of γ and can lead to unphysical results. Apparently, to obtain the complete description of crossover region we have to take into account non-commuting Magnus contributions.

6.2.3. Overdamped Regime

The situation changes qualitatively when

$$\Gamma_{\text{eff}} \gg \omega_0. \tag{118}$$

Neighboring sidebands overlap strongly and can no longer be regarded as independent coherent excitations.

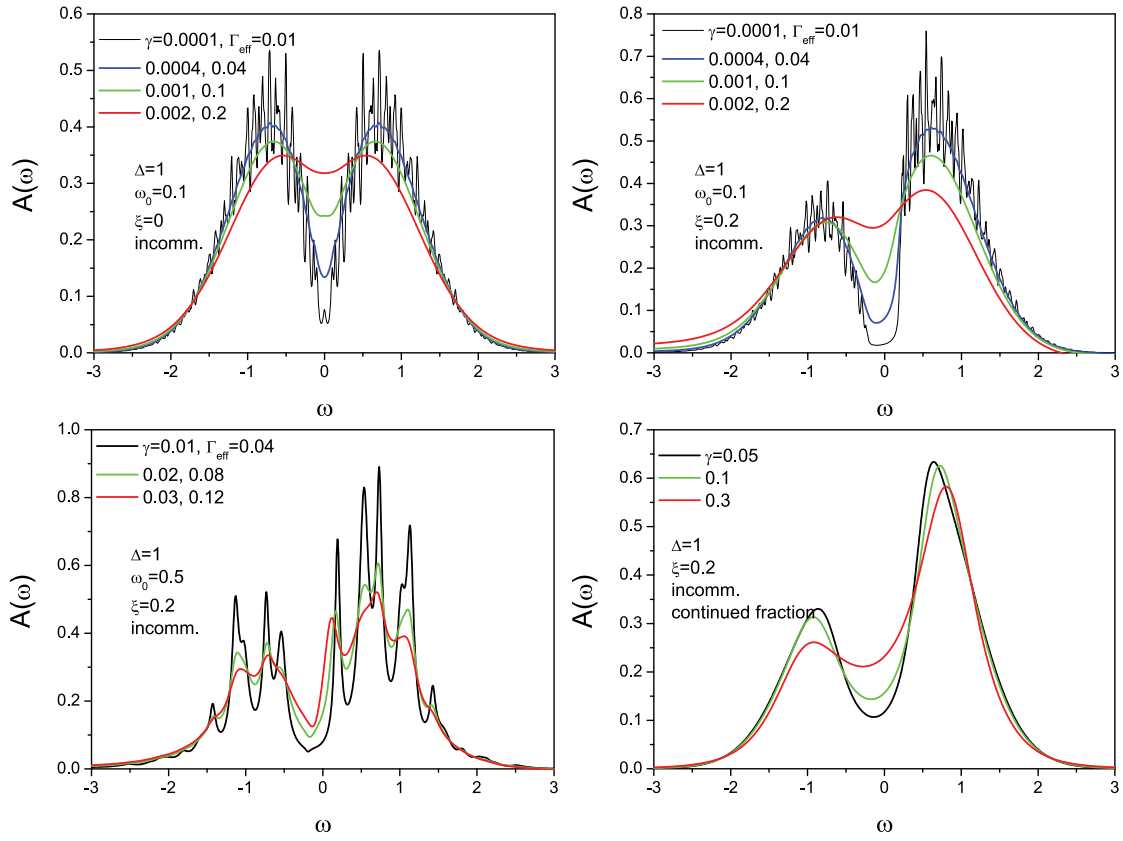

Fig. 4. Dependence of the spectral density for incommensurate case on γ for different values of ω_0 and ξ. The last panel shows spectral density dependence on γ in static ($\omega_0 = 0$) approximation obtained from exact continued fraction representation. All energies are given in units of Δ

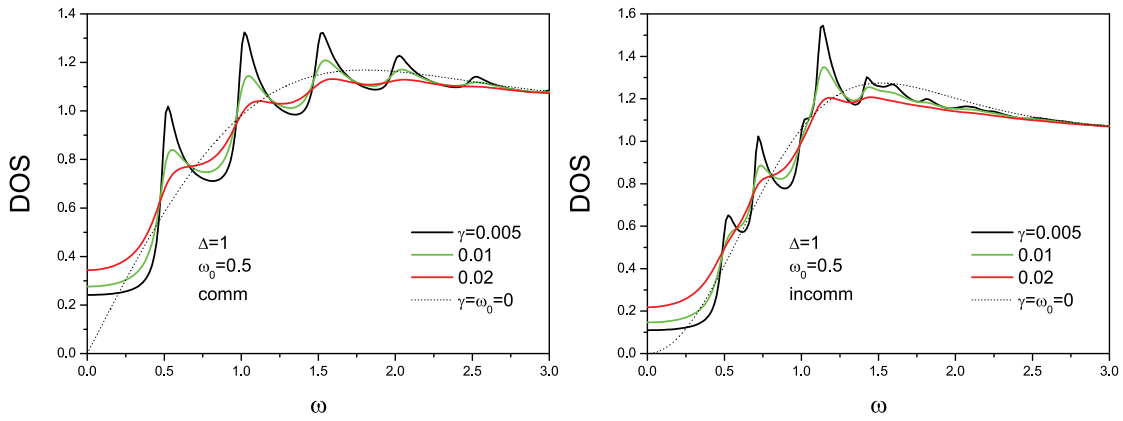

Fig. 5. Density of states (DOS), in units of the free-electron DOS, for commensurate (left) and incommensurate (right) cases and typical values of ω_0 and γ. Dotted lines represent exact behavior for static case $\omega_0 = 0$ and $\gamma = 0$ (Appendix D)

Although the mathematical series itself continues to converge because of the factorial suppression of the history weights, the physical interpretation in terms of coherent scattering histories becomes progressively less appropriate. However, in this case we can safely neglect ω_0 and use the continued-fraction solution for the static case instead, which correctly reproduces the spectral density behavior in the more or less trivial limit of large γ. Actually this is fully confirmed by the numerical results following from our double series expansion for the Green's function at large γ.

Thus the numerical results obtained in the present work suggest the following physical picture. When the fluctuating field oscillates sufficiently rapidly compared with its intrinsic decoherence rate, the electron is able to distinguish the individual dynamical scattering events. The corresponding spectrum consists of coherent dynamic sidebands. As decoherence increases, repeated scattering histories lose their mutual phase coherence. The electron no longer resolves the temporal structure of the fluctuating field and instead experiences transformation to effectively quasistatic ($\omega_0 = 0$) random gap.

7. PHYSICAL REALIZATIONS

The dynamic pseudogap model developed in the present work is intentionally formulated in a phenomenological manner. Its essential ingredients are a finite ordering wave vector $\mathbf{Q}$, a temporally fluctuating classical order parameter, and sufficiently strong electron scattering between nested portions of the Fermi surface. These ingredients naturally occur in a wide variety of correlated electron systems approaching density-wave instabilities.

7.1. Charge-Density-Wave Fluctuations

Perhaps the most direct realization of the present theory is provided by electronic systems close to a Peierls or CDW transition. Near the transition temperature the soft phonon mode associated with the ordering vector $\mathbf{Q}$ becomes strongly populated, $\omega_{\mathbf{Q}} \to 0$, and its occupation number

$$n_B(\omega_{\mathbf{Q}}) \simeq \frac{T}{\omega_{\mathbf{Q}}} \tag{119}$$

becomes very large. Under these conditions the lattice displacement may be treated as a classical stochastic field with finite temporal correlations $\Delta(t) = g_{\mathbf{Q}} u_{\mathbf{Q}}(t)$, where $u_{\mathbf{Q}}(t)$ denotes the slowly fluctuating soft phonon coordinate.

The phenomenological correlation function adopted throughout the present work,

$$\langle \Delta(t)\Delta^*(0)\rangle = \Delta^2 e^{-\gamma|t|}\cos(\omega_0 t), \tag{120}$$

may therefore be viewed as the effective long-time dynamics of a damped soft phonon mode.

More estimates of this kind are described in Appendix E.

7.2. Spin-Density-Wave Fluctuations

An analogous situation occurs near antiferromagnetic or SDW instabilities [11, 12, 17, 18, 32]. In this case the fluctuating order parameter represents slowly varying staggered magnetization,

$$\mathbf{M}(\mathbf{r}, t) = \mathbf{M}_Q(t) e^{i\mathbf{Q}\cdot\mathbf{r}} + \text{c.c.}, \tag{121}$$

which again produces repeated electronic scattering between nested regions of the Fermi surface. Provided the characteristic fluctuation frequency remains much smaller than the electronic bandwidth, the spin fluctuations may likewise be treated as an effectively classical random field.

7.3. Excitonic Insulator

The present formalism is equally applicable to systems approaching excitonic condensation [33]. Here the fluctuating order parameter corresponds to a transient electron-hole pairing amplitude $\Delta \sim \langle c_v^\dagger c_c\rangle$, whose temporal fluctuations produce a dynamic pseudogap in precisely the same manner as the CDW problem. Here the indices c and v denote conduction and valence band in a semimetal, with band extrema at points of Brillouin zone linked by nesting vector $\mathbf{Q}$.

7.4. Candidate Materials

Several classes of materials appear particularly well suited for the application of the present theory.

These include

- layered transition-metal dichalcogenides close to CDW ordering [34],
- quasi-one-dimensional Peierls systems [1],
- chromium and related itinerant antiferromagnets [32],
- underdoped cuprate superconductors exhibiting strong charge- or spin-density-wave fluctuations [2–4, 11–13, 17, 18],
- excitonic semimetals close to electronic ordering transitions [33].

In all these systems short-range order develops over a broad temperature range before true long-range ordering is established, producing precisely the fluctuating pseudogap regime described by the present model.

7.5. Angle-Resolved Photoemission

The most direct experimental signature of the coherent dynamic regime is expected in angle-resolved photoemission spectroscopy [35]. According to the present theory the spectral function consists of an infinite family of dynamically broadened sidebands separated by $\Delta\omega \sim \omega_0$. When $\omega_0 \gg \Gamma_{\text{eff}}$, individual sidebands remain partially resolved and should appear as satellite structures accompanying the principal quasiparticle peak.

As the effective decoherence increases these satellites broaden and merge, leading to the familiar pseudogap spectrum characteristic of the quasistatic fluctuating-gap regime.

8. CONCLUSIONS

In this work we have formulated a dynamic theory of pseudogap formation generated by finite-$\mathbf{Q}$ fluctuations possessing finite correlation time and characteristic oscillation frequency. Within the commuting (Abelian) approximation to the exact SU(2) time evolution we derived an explicit double-series representation of the single-particle Green's function describing coherent multiple scattering processes. The resulting propagator naturally acquires a generalized Bogoliubov structure in which every stochastic scattering history is characterized by an effective dynamic gap with complex Poisson distribution, giving an attractive physical picture of dynamic pseudogap formation.

A central result is the identification of the dynamically generated decoherence scale Γ_{eff}. The ratio $\omega_0/\Gamma_{\text{eff}}$ naturally separates two qualitatively different physical regimes. For $\omega_0 > \Gamma_{\text{eff}}$, electrons resolve the temporal dynamics of the fluctuating order parameter and the coherent double-series representation provides a controlled description of the resulting sideband structure. Conversely, when $\Gamma_{\text{eff}} \gtrsim \omega_0$, the electron loses phase coherence before resolving the oscillatory motion of the order parameter. The dynamic problem then crosses over to an effectively quasistatic regime described by the exact continued-fraction solution originally developed for static fluctuating-gap models. These two descriptions should therefore not be regarded as independent theories but rather as complementary asymptotic limits of one underlying dynamic pseudogap problem. The coherent double-series representation and the exact continued-fraction recursion derived in the present work should therefore be viewed as two complementary nonperturbative descriptions of the same dynamic pseudogap problem, with the crossover between them governed by the emergent decoherence scale Γ_{eff}.

Several exact results support the Green's function construction developed in the present work. For commensurate fluctuations at the Fermi surface ($\xi = 0$), where the Hamiltonians commute at different times, the coherent cumulant expansion becomes exact and reproduces the complete dynamic solution. In the opposite overdamped limit the exact continued-fraction recursion provides the correct quasistatic description. These two exact asymptotic limits strongly constrain the structure of the general theory and provide substantial justification for the coherent approximation over a broad physically relevant parameter range. Actually the agreement of our numerics with all known exact solutions of this model probably remains the main justification of our heuristic approach.

The principal approximation of the present work consists in neglecting the non-Abelian contributions generated by the SU(2) structure of the time-ordered evolution operator. These corrections are naturally organized by the Magnus expansion and are expected to become quantitatively important primarily in the crossover region $\omega_0 \sim \Gamma_{\text{eff}}$. At the same time, both analytical arguments and extensive numerical calculations indicate that the coherent approximation remains remarkably accurate over a wide range of model parameters, suggesting that higher Magnus terms mainly provide quantitative rather than qualitative corrections.

Further analysis of these difficulties is possible, in principle, by the use of special diagram technique for (pseudo)spin operators proposed in Refs. [23–27], which may become very useful for future developments of our theory.

Although formulated for classical Gaussian fluctuations, the present approach provides a natural starting point for more microscopic descriptions, based on different mechanisms of electron interactions with specific types of fluctuations at the edge of soft-mode phase transitions. The coherent double-series representation derived here may therefore be viewed as the simplest member of a broader class of non-Abelian fluctuating-gap theories describing dynamic electronic ordering phenomena. The future perspective requires additional and more deep analysis of the role of higher order contributions to Magnus expansion, which were dropped here in commuting approximation. This is actually the main limitation of the present theory which does not

allow the complete description of the crossover region from dynamic problem to static fluctuating gap model. At the same time we do not expect any drastic deviations from the physical picture described here.

The present formulation has been developed for fluctuations with a fixed nesting vector $\mathbf{Q}$ and therefore does not explicitly include spatial fluctuations of the ordering wave vector. A complete theory combining both temporal and spatial fluctuations remains an important problem for future investigations. Nevertheless, the close correspondence between the present dynamic theory and the earlier static fluctuating-gap models [6–18] suggests a simple phenomenological interpolation. In the static theories the inverse correlation length $\xi_{\rm corr}^{-1}$ enters the electronic Green's function through the effective damping $v_F/\xi_{\rm corr}$, where v_F is the Fermi velocity. This observation naturally motivates the introduction of the combined decoherence scale

$$\gamma_{\rm eff} = \gamma + \frac{v_F}{\xi_{\rm corr}}, \tag{122}$$

which simultaneously accounts for temporal and spatial loss of electronic coherence. Although phenomenological, this relation provides a plausible bridge between the present theory and future microscopic descriptions including both types of fluctuations.

Finally, the present work establishes a unified physical picture of dynamic pseudogap formation continuously connecting coherent dynamic sideband physics, quasistatic fluctuating-gap behavior, and the motional-narrowing limit within a single microscopic framework. We hope that this approach will provide a useful basis for future extensions incorporating spatial fluctuations, non-Abelian corrections, and microscopic models of soft collective modes, as well as for quantitative comparison with angle-resolved photoemission, tunneling spectroscopy, optical conductivity, and other experimental probes of fluctuating electronic order.

Acknowledgements. The authors are grateful to an anonymous referee for constructive criticism and valuable suggestions to improve the initial version of the paper.

Funding. This work was supported by ongoing institutional funding. No additional grants to carry out this particular research were obtained.

Conflict of interest. The authors declare that they have no conflict of interest.

Authors' contributions. The contributions of the authors are equal.

APPENDIX A
KELDYSH FORMALISM

The time dependence of the fluctuating order parameter makes the conventional equilibrium Green's function formalism rather limited. Instead, the natural framework is provided by the non-equilibrium Keldysh technique, in which the electron propagator is defined on the closed real-time contour. Below we show how our dynamic pseudogap problem can be reformulated using Keldysh formalism.

We shall also present the general derivation of the dynamic double-series Green's function used in the main part of the text directly from the Keldysh contour formulation. The purpose of this derivation is to make explicit how the stochastic history indices (n, m) and their complex Poisson weights arise from the underlying Gaussian scattering diagrams, and how the finite-Q Nambu structure produces the generalized Bogoliubov denominator.

A.1. Microscopic Hamiltonian and Nambu Representation

The contour-ordered Green's function is defined by

$$G(1,2) = -i\left\langle T_C \psi(1)\psi^\dagger(2)\right\rangle, \tag{A1}$$

where T_C denotes ordering along the Keldysh contour.

Introducing Nambu spinors

$$\hat{\Psi}_{\mathbf{k}}(t) = \begin{pmatrix} c_{\mathbf{k}}(t) \\ c_{\mathbf{k}+\mathbf{Q}}(t) \end{pmatrix}, \tag{A2}$$

the Hamiltonian assumes the compact matrix form

$$H(t) = \sum_{\mathbf{k}} \hat{\Psi}^\dagger_{\mathbf{k}} \hat{H}(t) \hat{\Psi}_{\mathbf{k}}, \tag{A3}$$

with

$$\hat{H}(t) = \xi_k \sigma_3 + \Delta(t)\sigma_+ + \Delta^*(t)\sigma_-, \tag{A4}$$

where σ_i are the Pauli matrices. The important point is that σ_i act only in the two-dimensional $\mathbf{k}, \mathbf{k}+\mathbf{Q}$ space. They are ordinary c-number matrices and the underlying particles remain canonical fermions.

The Keldysh generating functional is

$$Z = \int \mathcal{D}(\hat{\Psi}^\dagger, \hat{\Psi}) \mathcal{D}\Delta\, \mathcal{P}[\Delta]\, e^{iS[\hat{\Psi}^\dagger, \hat{\Psi}, \Delta]}, \tag{A5}$$

where

$$S = S_0 + S_{\rm int} \tag{A6}$$

is the action on the Keldysh contour.

The electronic part is

$$S_0 = \int\limits_C dt \sum_{\mathbf{k}} \hat{\Psi}^\dagger_{\mathbf{k}} \left(i\partial_t - \xi_{\mathbf{k}}\sigma_3 \right) \hat{\Psi}_{\mathbf{k}}, \tag{A7}$$

while

$$S_{\rm int} = -\int\limits_C dt \sum_{\mathbf{k}} \hat{\Psi}^\dagger_{\mathbf{k}} \left[\Delta(t)\sigma_+ + \Delta^*(t)\sigma_- \right] \hat{\Psi}_{\mathbf{k}}. \tag{A8}$$

Since the fluctuating field is Gaussian, the functional integration over $\Delta(t)$ can be carried out exactly. Using the standard Gaussian identity

$$\int \mathcal{D}\Delta \, \exp\left[-\Delta^\dagger K \Delta + J^\dagger \Delta + \Delta^\dagger J \right] = \\ = (\det K)^{-1} \exp\left(J^\dagger D J \right), \tag{A9}$$

where $D = K^{-1}$ is time correlation function along the Keldysh contour, one immediately obtains

$$Z = \int \mathcal{D}(\hat{\Psi}^\dagger, \hat{\Psi}) \, e^{iS_{\rm eff}}, \tag{A10}$$

with the exact effective electronic action

$$S_{\rm eff} = S_0 + S_{\rm ind}, \tag{A11}$$

where

$$S_{\rm ind} = -\int\limits_C dt dt' \, D(t-t') \times \\ \times \sum_{\mathbf{k}\mathbf{k}'} \left[\hat{\Psi}^\dagger_{\mathbf{k}}(t)\sigma_+ \hat{\Psi}_{\mathbf{k}}(t) \right] \left[\hat{\Psi}^\dagger_{\mathbf{k}'}(t')\sigma_- \hat{\Psi}_{\mathbf{k}'}(t') \right]. \tag{A12}$$

Now the fluctuating order parameter has disappeared completely, being replaced by a retarded nonlocal electron–electron interaction mediated by the correlation function of the stochastic field.

Several important observations follow immediately. First, the effective interaction is nonlocal in time. Unlike the static theory, the electron retains memory of its previous scattering events over a time interval determined by the correlation function $D(t)$. Second, all information concerning the fluctuating order parameter enters only through its two-time correlation function. This remarkable simplification follows directly from the Gaussian nature of the stochastic process. Finally, Eq. (A12) is exact. No perturbative approximation has yet been introduced. The only assumption employed thus far is the Gaussian statistics of the fluctuating order parameter.

Throughout the present work the fluctuating pseudogap field has been treated as a classical Gaussian stochastic process characterized by the correlation function

$$\langle \Delta(\mathbf{r}, t) \Delta^*(\mathbf{r}', t') \rangle = D(\mathbf{r} - \mathbf{r}', t - t'). \tag{A13}$$

In the simplified model considered in the main text the spatial correlations were neglected.

We have seen above that assuming fluctuating field Gaussian, we may integrate it out exactly to obtain effective action (A12), where

$$D_C(t_1, t_2) = -i \left\langle T_C \Delta(t_1) \Delta^*(t_2) \right\rangle \tag{A14}$$

is the contour propagator of the fluctuating order parameter. The contour Green's function may be decomposed into the standard Keldysh components,

$$D_C \Longrightarrow \left(D^R, D^A, D^K \right), \tag{A15}$$

where D^R and D^A describe the causal response of the order parameter, while D^K determines the fluctuation spectrum.

The present model corresponds to the classical limit in which the order parameter is treated as an external stochastic field. In equilibrium we have fluctuation-dissipation theorem:

$$D^K(\omega) = \left[D^R(\omega) - D^A(\omega) \right] \mathrm{cth}\left(\frac{\omega}{2T} \right), \tag{A16}$$

so that for $T \gg \omega$ we have $\mathrm{cth}(\omega/2T) \approx 2T/\omega \gg 1$ and $D^K(\omega) \gg D^{R,A}(\omega)$. In this case the Keldysh component

$$D^K(t) \propto \langle \Delta(t) \Delta^*(0) \rangle \tag{A17}$$

dominates and governs electron dynamics, whereas the retarded and advanced components actually do not play any role due to the classical nature of our random field. Actually the exponential damping of the electronic Green's function does not arise from phenomenological broadening but from averaging over all realizations of the fluctuating pseudogap field.

A.2. Gaussian Field Contractions

Introduce the Keldysh contour C and define

$$\hat{G}_C(1,2) = -i \left\langle T_C \hat{\Psi}(1) \hat{\Psi}^\dagger(2) \right\rangle_\Delta, \tag{A18}$$

where the average is over the classical fluctuating field.

For a fixed realization of $\Delta(t)$,

$$\left[i\partial_{t_1} - \hat{H}(t_1) \right] \hat{G}_C(1,2) = \delta_C(1-2). \tag{A19}$$

Define

$$\hat{G}_{0C}^{-1} = i\partial_t - \xi\sigma_3. \tag{A20}$$

The contour Dyson equation is therefore

$$\hat{G}_C = \hat{G}_{0C} + \hat{G}_{0C}\hat{V}\hat{G}_C, \tag{A21}$$

with

$$\hat{V}(t) = \Delta(t)\sigma_+ + \Delta^*(t)\sigma_-. \tag{A22}$$

Iterating Eq. (A21) gives

$$\hat{G}_C = \hat{G}_{0C} + \hat{G}_{0C}\hat{V}\hat{G}_{0C} + \hat{G}_{0C}\hat{V}\hat{G}_{0C}\hat{V}\hat{G}_{0C} + \\ + \hat{G}_{0C}\hat{V}\hat{G}_{0C}\hat{V}\hat{G}_{0C}\hat{V}\hat{G}_{0C} + \cdots. \tag{A23}$$

This is the starting point for the Keldysh diagrammatic expansion.

The classical field has zero mean,

$$\langle\Delta(t)\rangle = 0, \tag{A24}$$

and correlation function

$$D_C(t,t') = \langle\Delta(t)\Delta^*(t')\rangle_C. \tag{A25}$$

For the incommensurate case,

$$\langle\Delta(t)\Delta(t')\rangle = 0, \tag{A26}$$

while

$$D(t-t') = \Delta^2 e^{-\gamma|t-t'|}\cos[\omega_0(t-t')]. \tag{A27}$$

The Gaussian nature of the classical field means that its higher moments are reduced by ordinary Gaussian Wick contraction,

$$\langle\Delta_1\Delta_2\Delta_3^*\Delta_4^*\rangle = D_{12}D_{34} + D_{14}D_{32}, \tag{A28}$$

and similarly at higher order. It is simply Wick's theorem for the classical Gaussian random field. Every pair of field vertices in the electronic Dyson series is therefore joined by a contour disorder line D_C.

The retarded electronic Green's function is given by

$$\hat{G}^R(\epsilon,\xi) = \left[\epsilon + i0 - \xi\sigma_3 - \hat{\Sigma}^R(\epsilon,\xi)\right]^{-1}. \tag{A29}$$

The self-energy generated by the classical field has the schematic Keldysh form

$$\hat{\Sigma}^R = \int\frac{d\Omega}{2\pi}\Big[D^K(\Omega)\sigma_a\hat{G}^R(\epsilon-\Omega,\xi)\sigma_a + \\ + D^R(\Omega)\sigma_a\hat{G}^K(\epsilon-\Omega,\xi)\sigma_a\Big]. \tag{A30}$$

For a prescribed classical stochastic field the dominant noise contribution may be represented as

$$\hat{\Sigma}^R_{\rm cl} \simeq \int\frac{d\Omega}{2\pi}D^K(\Omega)\sigma_a\hat{G}^R(\epsilon-\Omega,\xi)\sigma_a. \tag{A31}$$

Equation (A31) displays the fundamental separation of variables. The noise spectrum is independent of ξ, whereas the electronic propagator appearing inside the convolution depends explicitly on ξ.

A.3. The Finite-Q Pseudospin Structure of the Diagrams

The free propagator is

$$\hat{G}_{0C}^{-1}(\omega) = \omega\sigma_0 - \xi\sigma_3. \tag{A32}$$

Consequently,

$$\hat{G}_{0C}(\omega,\xi) = \frac{\omega\sigma_0 + \xi\sigma_3}{\omega^2 - \xi^2}. \tag{A33}$$

The scattering vertices are off diagonal:

$$V_+ = \sigma_+, \qquad V_- = \sigma_-. \tag{A34}$$

Using

$$\sigma_\pm\sigma_3 = \mp\sigma_3\sigma_\pm, \tag{A35}$$

one obtains

$$\sigma_\pm\hat{G}_0(\xi) = \hat{G}_0(-\xi)\sigma_\pm. \tag{A36}$$

Thus every scattering event changes the branch,

$$\xi \longrightarrow -\xi \longrightarrow \xi \longrightarrow -\xi\cdots. \tag{A37}$$

This branch alternation is the microscopic origin of the Nambu – Bogoliubov structure. It is already present before any stochastic averaging is performed.

For positive time difference,

$$D(t) = \frac{\Delta^2}{2}e^{-\gamma t}\left(e^{-i\omega_0 t} + e^{+i\omega_0 t}\right). \tag{A38}$$

It is convenient to introduce two elementary dynamic propagators,

$$D_+(t) = \frac{\Delta^2}{2}e^{-(\gamma+i\omega_0)t}, \tag{A39}$$

and

$$D_-(t) = \frac{\Delta^2}{2}e^{-(\gamma-i\omega_0)t}. \tag{A40}$$

The complete diagram series can consequently be classified according to the number of D_+ and D_- lines occurring in a scattering history. We denote these numbers by

$$n = 0,1,2,\ldots, \qquad m = 0,1,2,\ldots. \tag{A41}$$

The pair (n,m) is therefore a dynamic history index.

Consider first a sequence of n identical D_+ insertions. Because each D_+ is exponential, the ordered contour integral has the generic form

$$I_n^{(+)}(t) = \int\limits_{0<t_n<\cdots<t_1<t} dt_1\cdots dt_n\prod_{j=1}^{n}e^{-\Omega_+(t_j-t_{j+1})}, \tag{A42}$$

where

$$t_{n+1} = 0, \qquad \Omega_+ = \gamma + i\omega_0. \tag{A43}$$

Introduce the interval variables

$$\tau_j = t_j - t_{j+1}. \tag{A44}$$

The ordered domain becomes

$$\tau_j \geq 0, \qquad \sum_{j=1}^{n} \tau_j \leq t. \tag{A45}$$

The integral is consequently generated recursively. Defining

$$A_n^{(+)} \tag{A46}$$

as the coefficient of the corresponding history, one obtains

$$A_n^{(+)} = \frac{\Delta^2/2}{\Omega_+} \frac{1}{n} A_{n-1}^{(+)}. \tag{A47}$$

Hence

$$A_n^{(+)} = \frac{1}{n!} \left(\frac{\Delta^2}{2\Omega_+^2} \right)^n. \tag{A48}$$

The same construction for the opposite oscillatory component gives

$$A_m^{(-)} = \frac{1}{m!} \left(\frac{\Delta^2}{2\Omega_-^2} \right)^m, \tag{A49}$$

where

$$\Omega_- = \gamma - i\omega_0. \tag{A50}$$

Thus the factorials in the Poisson weights arise directly from the ordered Keldysh time integrations.

For a general (n, m) sector, adding one additional D_+ or D_- line gives

$$A_{nm} = \frac{\Delta^2}{2} \frac{A_{n-1,m}/\Omega_+ + A_{n,m-1}/\Omega_-}{n\Omega_+ + m\Omega_-}. \tag{A51}$$

The boundary condition is

$$A_{00} = 1, \tag{A52}$$

and

$$A_{n<0,m} = A_{n,m<0} = 0. \tag{A53}$$

The solution of Eq. (A51) is

$$A_{nm} = e^{-\lambda_1 - \lambda_2} \frac{\lambda_1^n}{n!} \frac{\lambda_2^m}{m!}, \tag{A54}$$

where λ_1 and λ_2 were defined in Eq. (58) of the main text. The exponential prefactor follows from the sum of disconnected repetitions of the elementary histories.

Thus the entire Gaussian Keldysh diagram series has been reorganized into

$$\sum_{n,m} P_{\lambda_1}(n) P_{\lambda_2}(m) \times \\ \times [\text{Nambu propagator of history } (nm)]. \tag{A55}$$

The procedure described here presents an alternative derivation of our Poisson averaged histories approach used in the main part of the text.

This derivation implicitly assumed that diagrams differing only by permutations of equivalent D_+ and D_- insertions can be grouped into the same history sector. In the exact finite-Q theory this is not generally allowed. For example, consider two successive transverse scattering operations. Their two possible orderings contain

$$\sigma_+ \sigma_- \tag{A56}$$

and

$$\sigma_- \sigma_+, \tag{A57}$$

whose difference is

$$[\sigma_+, \sigma_-] = \sigma_3. \tag{A58}$$

The Abelian approximation amounts to dropping precisely this ordering-sensitive difference. Diagrammatically,

$$D_+ D_- \quad \leftrightarrow \quad D_- D_+ \tag{A59}$$

are assigned the same history amplitude.

The approximation therefore concerns the ordering of the pseudospin vertices, not the stochastic Gaussian contractions themselves.

A.4. History Hamiltonian

After the Gaussian diagrams have been grouped into an (n, m) sector, the remaining electronic object is a two-component propagator. Consider the commensurate case. The dynamic phase accumulated by the history is

$$\Omega_{nm} = (n - m)\omega_0 - i(n + m)\gamma. \tag{A60}$$

The nonperturbative damping generated by the repeated dynamic scattering is denoted by

$$\Gamma_{\text{eff}} = \frac{\gamma\Delta^2}{\omega_0^2 + \gamma^2}. \tag{A61}$$

Within the Abelian history construction the corresponding complex transverse gap is

$$\Delta_{nm} = (n - m)\omega_0 - i(n + m)\gamma - i\Gamma_{\text{eff}}. \tag{A62}$$

Equivalently,

$$\Delta_{nm} = (\omega_0 - i\gamma)(n - \lambda_1) + (-\omega_0 - i\gamma)(m - \lambda_2). \quad \text{(A63)}$$

The history Hamiltonian is therefore assumed to be

$$\hat{H}_{nm} = \xi\sigma_3 + \Delta_{nm}\sigma_1. \quad \text{(A64)}$$

This step is the finite-Q part of the construction: the dynamic history does not produce a scalar shift of ξ. It produces a transverse matrix element connecting the two nested electronic branches.

The Green's function associated with a fixed history for commensurate case satisfies

$$\left[\omega\sigma_0 - \hat{H}_{nm}\right]\hat{G}_{nm} = \sigma_0. \quad \text{(A65)}$$

Using Eq. (A64),

$$\left[\omega\sigma_0 - \xi\sigma_3 - \Delta_{nm}\sigma_1\right]\hat{G}_{nm} = \sigma_0. \quad \text{(A66)}$$

Since

$$\{\sigma_1, \sigma_3\} = 0, \quad \text{(A67)}$$

we have

$$(\xi\sigma_3 + \Delta_{nm}\sigma_1)^2 = \xi^2 + \Delta_{nm}^2. \quad \text{(A68)}$$

Consequently,

$$\hat{G}_{nm} = \frac{\omega\sigma_0 + \xi\sigma_3 + \Delta_{nm}\sigma_1}{\omega^2 - \xi^2 - \Delta_{nm}^2}. \quad \text{(A69)}$$

The physical electron component is

$$G_{nm,11}(\omega, \xi) = \frac{\omega + \xi}{\omega^2 - \xi^2 - \Delta_{nm}^2}. \quad \text{(A70)}$$

Thus the pseudogap appears directly from the off-diagonal finite-Q scattering vertex.

Combining the Gaussian history amplitude Eq. (A54) with the history-resolved Nambu propagator Eq. (A69), we obtain

$$\hat{G}(\omega, \xi) = \\ = e^{-\lambda_1 - \lambda_2} \sum_{n,m=0}^{\infty} \frac{\lambda_1^n}{n!}\frac{\lambda_2^m}{m!}\frac{\omega\sigma_0 + \xi\sigma_3 + \Delta_{nm}\sigma_1}{\omega^2 - \xi^2 - \Delta_{nm}^2}. \quad \text{(A71)}$$

The physical electron Green function is therefore

$$G(\omega, \xi) = \\ = e^{-\lambda_1 - \lambda_2} \sum_{n,m=0}^{\infty} \frac{\lambda_1^n}{n!}\frac{\lambda_2^m}{m!}\frac{\omega + \xi}{\omega^2 - \xi^2 - \Delta_{nm}^2}. \quad \text{(A72)}$$

This expression is obtained here directly by reorganizing the Keldysh Dyson series and its Gaussian field contractions.

The structure of Eq. (A72) can be understood directly from the diagrams. At zero scattering order,

$$G^{(0)} = \frac{1}{\omega - \xi + i0}. \quad \text{(A73)}$$

At second order, the elementary contribution contains

$$G_0(\xi), \sigma_+ G_0(-\xi), \sigma_- G_0(\xi) \quad \text{(A74)}$$

multiplied by one field contraction D_C. At fourth order one obtains

$$G^{(4)} \sim G_0\sigma_+ G_0\sigma_- G_0\sigma_+ G_0\sigma_- G_0 \left[D_{12}D_{34} + D_{14}D_{32}\right]. \quad \text{(A75)}$$

The two Gaussian pairings correspond to the two topologically distinct contractions.

At arbitrary order, the Gaussian contractions generate all pairings of the field vertices. The Abelian approximation identifies all diagrams having the same numbers (n, m) of the two elementary dynamical components. Their sum is precisely represented by the history amplitude

$$P_{\lambda_1}(n)P_{\lambda_2}(m). \quad \text{(A76)}$$

Thus Eq. (A72) is not a phenomenological ansatz: it is the compact representation of the Abelianized infinite Keldysh diagram series.

For the commensurate case,

$$\Delta = \Delta^*, \quad \text{(A77)}$$

and the construction above directly gives the Abelian history Hamiltonian

$$\hat{H}_{nm} = \xi\sigma_3 + \Delta_{nm}\sigma_1. \quad \text{(A78)}$$

At $\xi = 0$,

$$\hat{H}(t) = \Delta(t)\sigma_1, \quad \text{(A79)}$$

so

$$[\hat{H}(t_1), \hat{H}(t_2)] = 0 \quad \text{(A80)}$$

identically. The Abelian construction is therefore exact in this limit.

For the incommensurate case,

$$\Delta(t) = \Delta_1(t) + i\Delta_2(t), \quad \text{(A81)}$$

and

$$\hat{H}(t) = \xi\sigma_3 + \Delta_1(t)\sigma_1 + \Delta_2(t)\sigma_2. \quad \text{(A82)}$$

The corresponding Abelian history construction introduces

$$\hat{H}_{nm} = \xi\sigma_3 + \Delta_{1,n}\sigma_1 + \Delta_{2,m}\sigma_2, \quad \text{(A83)}$$

with

$$\Delta_{1,n} = (\omega_0 - i\gamma)(n - \lambda_1), \tag{A84}$$

$$\Delta_{2,m} = (-\omega_0 - i\gamma)(m - \lambda_2). \tag{A85}$$

Hence

$$\hat{H}^2_{nm} = \left[\xi^2 + \Delta^2_{1,n} + \Delta^2_{2,m}\right]\sigma_0, \tag{A86}$$

and

$$G_{nm,11} = \frac{\omega + \xi}{\omega^2 - \xi^2 - \Delta^2_{1,n} - \Delta^2_{2,m}}. \tag{A87}$$

The Gaussian history weights remain

$$P_{\lambda_1}(n)P_{\lambda_2}(m). \tag{A88}$$

For this incommensurate construction, however, one must explicitly state that the matrix history assignment is an Abelian $O(2)$ extension rather than an exact solution of the full non-Abelian Keldysh problem.

The discarded contributions can be identified explicitly. Consider two transverse vertices,

$$V_+ = \Delta\sigma_+, \qquad V_- = \Delta^*\sigma_-. \tag{A89}$$

The two possible orderings differ by

$$V_+V_- - V_-V_+ = |\Delta|^2[\sigma_+, \sigma_-] = |\Delta|^2\sigma_3. \tag{A90}$$

In the exact Keldysh series these two orderings correspond to distinct pseudospin histories. The Abelian construction replaces

$$V_+V_- \quad \text{and} \quad V_-V_+ \tag{A91}$$

by their common commuting history contribution. Thus the approximation is precisely

$$[\sigma_+, \sigma_-] \to 0 \tag{A92}$$

inside the history resummation. Importantly, we do not set

$$\sigma_\pm \to 0. \tag{A93}$$

The transverse scattering vertices remain and are responsible for the pseudogap. This observation provides the natural starting point for a systematic non-Abelian extension.

APPENDIX B
COMMENSURATE AND INCOMMENSURATE FLUCTUATIONS

B.1. Real Fluctuating Order Parameter

For a commensurate charge-density wave the order parameter may be chosen real, and the interaction Hamiltonian takes the form

$$H_{\rm int}(t) = \Delta(t)\sigma_1. \tag{B1}$$

The perturbation expansion therefore involves only a single fluctuating Gaussian field with correlation function

$$\langle\Delta(t_1)\Delta(t_2)\rangle = D(t_1 - t_2). \tag{B2}$$

All interaction vertices are identical, and every Wick contraction involves the same scalar propagator.

The square of interaction Hamiltonian reduces to

$$H^2_{\rm int} = \Delta^2\,\mathbf{1}, \tag{B3}$$

leading to the single effective history-dependent gap discussed in the main text.

B.2. Complex Fluctuating Order Parameter

For an incommensurate density wave the order parameter is intrinsically complex,

$$\Delta = \Delta_1 + i\Delta_2, \tag{B4}$$

and the interaction Hamiltonian may be written as

$$H_{\rm int}(t) = \Delta_1(t)\sigma_1 + \Delta_2(t)\sigma_2. \tag{B5}$$

The perturbation expansion now contains two statistically independent Gaussian fields.

Assuming isotropic Gaussian fluctuations, the elementary correlator becomes

$$\langle\Delta_a(t_1)\Delta_b(t_2)\rangle = \delta_{ab}D(t_1 - t_2), \qquad a, b = 1, 2. \tag{B6}$$

Equation (B6) immediately implies that Wick contractions preserve the component index of the fluctuating field. Mixed contractions between Δ_1 and Δ_2 vanish identically.

Consequently, the perturbation expansion naturally separates into two independent contraction families. Within the dynamic double-series representation these two families are naturally labelled by the stochastic history indices n and m.

The decomposition employed above follows directly from the standard electron–density-wave interaction Hamiltonian. For an incommensurate charge- density wave the interaction with the fluctuating order parameter is naturally written as

$$H_{\rm int}(t) = \Delta(t)\sigma_+ + \Delta^*(t)\sigma_-. \tag{B7}$$

Writing the complex order parameter as

$$\Delta = \Delta_1 + i\Delta_2, \qquad \Delta^* = \Delta_1 - i\Delta_2, \tag{B8}$$

one immediately obtains

$$\begin{aligned} H_{\rm int} &= (\Delta_1 + i\Delta_2)\sigma_+ + (\Delta_1 - i\Delta_2)\sigma_- = \\ &= \Delta_1(\sigma_+ + \sigma_-) + i\Delta_2(\sigma_+ - \sigma_-). \end{aligned} \tag{B9}$$

Using the identities

$$\sigma_+ + \sigma_- = \sigma_1, \qquad i(\sigma_+ - \sigma_-) = -\sigma_2, \tag{B10}$$

one finally arrives at

$$H_{\rm int} = \Delta_1\sigma_1 - \Delta_2\sigma_2. \tag{B11}$$

The relative sign depends only upon the convention chosen for the definition of $\sigma_\pm$ or, equivalently, for the phase of the complex order parameter, and therefore has no physical significance. The important point is that the two real components of the complex order parameter couple to two mutually anticommuting Pauli matrices.

The square of the interaction Hamiltonian therefore becomes

$$H_{\rm int}^2 = \Delta_1^2\sigma_1^2 + \Delta_2^2\sigma_2^2 - \Delta_1\Delta_2(\sigma_1\sigma_2 + \sigma_2\sigma_1). \tag{B12}$$

Using

$$\sigma_1^2 = \sigma_2^2 = \mathbf{1}, \qquad \{\sigma_1, \sigma_2\} = 0, \tag{B13}$$

one obtains

$$H_{\rm int}^2 = (\Delta_1^2 + \Delta_2^2)\mathbf{1}. \tag{B14}$$

Equation (B14) demonstrates that the spectrum of our model depends only upon the rotationally invariant quadratic form $\Delta^2 = \Delta_1^2 + \Delta_2^2$.

B.3. Possible Generalizations

The above construction suggests that the dynamic double-series formalism is largely independent of the internal symmetry of the fluctuating order parameter. Instead, the symmetry enters through the matrix algebra associated with the interaction Hamiltonian.

For example, a three-component fluctuating order parameter may formally be written as

$$H_{\rm int} = \sum_{a=1}^{3} \Delta_a\sigma_a, \tag{B15}$$

which immediately gives

$$H_{\rm int}^2 = \sum_{a=1}^{3} \Delta_a^2\,\mathbf{1}. \tag{B16}$$

This observation suggests that the history Green's function may generally be constructed from the invariant quadratic form associated with the internal symmetry of the fluctuating order parameter. In this sense, the dynamic double-series representation appears to be universal, while different physical systems correspond to different realizations of the underlying algebra.

The above considerations are intended only as an algebraic interpretation of the proposed history Green's functions. A complete microscopic derivation for general multicomponent order parameters remains an interesting subject for future investigation.

APPENDIX C
MAGNUS EXPANSION AND NON-ABELIAN STOCHASTIC SU(2) EVOLUTION

C.1. Time Evolution and Magnus Terms

The exact time evolution operator is

$$U(t) = T\exp\left[-i\int_0^t dt'\,H(t')\right]. \tag{C1}$$

Interaction operators at different times in general do not commute,

$$[H(t_1), H(t_2)] \neq 0. \tag{C2}$$

The evolution operator may now be written as

$$U(t) = \exp\left[\Omega_1 + \Omega_2 + \Omega_3 + \cdots\right], \tag{C3}$$

where

$$\Omega_1 = -i\int_0^t dt_1\,H(t_1) \tag{C4}$$

is the Abelian contribution.

The leading non-Abelian correction is

$$\Omega_2 = -\frac{1}{2}\int_0^t dt_1\int_0^{t_1} dt_2\,[H(t_1), H(t_2)]. \tag{C5}$$

C.2. Commensurate versus Incommensurate Order

An important qualitative difference between commensurate and incommensurate dynamic pseudogap fluctuations appears already at the level of the Magnus expansion.

For the commensurate model discussed in the main text, the Nambu Hamiltonian is

$$\hat{H}(t) = \xi\sigma_3 + \Delta(t)\sigma_1, \tag{C6}$$

where the fluctuating field $\Delta(t)$ is real.

The second Magnus term is controlled by

$$[\hat{H}(t_1), \hat{H}(t_2)] = 2i\xi\,[\Delta(t_2) - \Delta(t_1)]\,\sigma_2. \tag{C7}$$

Therefore

$$\xi = 0 \qquad \Longrightarrow \qquad [\hat{H}(t_1), \hat{H}(t_2)] = 0, \tag{C8}$$

so that all higher Magnus terms vanish identically,

$$\Omega_2 = \Omega_3 = \cdots = 0. \tag{C9}$$

Consequently, at the Fermi surface the cumulant solution becomes exact, because the Hamiltonians at different times commute.

The static contribution $\xi\sigma_3$ acts as a pseudomagnetic field directed along the third axis of SU(2) space, whereas $\Delta(t)\sigma_1$ represents a time-dependent field directed along the first axis. Because these two pseudomagnetic fields are not parallel, successive infinitesimal rotations occur about different axes. The resulting evolution depends on the order in which the rotations are performed, producing the Magnus commutators. At the Fermi surface the static component disappears, leaving only the time-dependent field along a single SU(2) axis. All infinitesimal rotations then commute identically.

For incommensurate order the situation changes qualitatively. The Hamiltonian is now

$$\hat{H}(t) = \xi\sigma_3 + \Delta(t)\sigma_+ + \Delta^*(t)\sigma_-, \tag{C10}$$

or equivalently

$$\hat{H}(t) = \xi\sigma_3 + \Delta_1(t)\sigma_1 + \Delta_2(t)\sigma_2, \tag{C11}$$

where

$$\Delta(t) = \Delta_1(t) + i\Delta_2(t). \tag{C12}$$

Then one obtains

$$\begin{aligned}[\hat{H}(t_1), \hat{H}(t_2)] = {} & 2i\xi\left[\Delta_1(t_2) - \Delta_1(t_1)\right]\sigma_2 - \\ & - 2i\xi\left[\Delta_2(t_2) - \Delta_2(t_1)\right]\sigma_1 + \\ & + 2i\Big[\Delta_1(t_1)\Delta_2(t_2) - \Delta_2(t_1)\Delta_1(t_2)\Big]\sigma_3. \end{aligned} \tag{C13}$$

Unlike the commensurate case, the last contribution survives even exactly at the Fermi surface ($\xi = 0$), giving

$$\begin{aligned}[\hat{H}(t_1), \hat{H}(t_2)] = {} & \\ & = 2i\Big[\Delta_1(t_1)\Delta_2(t_2) - \Delta_2(t_1)\Delta_1(t_2)\Big]\sigma_3. \end{aligned} \tag{C14}$$

Therefore

$$\Omega_2 \neq 0 \qquad (\xi = 0) \tag{C15}$$

for generic incommensurate fluctuations.

Equation (C14) admits a simple geometric interpretation. Introducing the two-dimensional vector order parameter as

$$\boldsymbol{\Delta}(t) = \left(\Delta_1(t), \Delta_2(t)\right), \tag{C16}$$

the commutator may be written as

$$[\hat{H}(t_1), \hat{H}(t_2)] = 2i\left[\boldsymbol{\Delta}(t_1) \times \boldsymbol{\Delta}(t_2)\right]\sigma_3. \tag{C17}$$

The second Magnus term is therefore proportional to the oriented area spanned by the order parameter during its stochastic evolution at two different times in the complex order-parameter plane.

This result demonstrates that the noncommutativity of the incommensurate problem has a purely geometric origin. Although the fluctuating field is classical, the pseudospin Hamiltonian rotates about different axes in SU(2) space at different times. Consequently, the time-evolution operators do not commute even at the Fermi surface.

By contrast, in the commensurate model the fluctuating field is purely real, so all Hamiltonians become proportional to the same generator σ_1 when $\xi = 0$. The dynamics then becomes effectively Abelian and the Magnus expansion terminates after the first term.

APPENDIX D
THE LIMIT OF $\gamma = 0$, $\omega_0 \to 0$

For the case of incommensurate fluctuations (complex order parameter) the double series for the Green's functions in the limit of $\gamma = 0$ and $\omega_0 \ll \Delta$ can be written as

$$\begin{aligned} G(\omega, \xi) = {} & \sum_{n,m=0}^{\infty} P_{\lambda_1}(n) P_{\lambda_2}(m) \times \\ & \times \frac{\omega + \xi}{\omega^2 - \xi^2 - \omega_0^2(n - \lambda_1)^2 - \omega_0^2(m - \lambda_2)^2}, \end{aligned} \tag{D1}$$

where $\lambda_i = \Delta^2/2\omega_0^2 \gg 1$ and the complex Poisson distributions reduce to the Gaussian form:

$$P_{\lambda_i}(k) = \frac{\omega_0}{\sqrt{\pi}\Delta} \exp\left[-\frac{\omega_0^2(k - \Delta^2/2\omega_0^2)^2}{\Delta^2}\right]. \tag{D2}$$

Then introducing $x = n - \Delta^2/2\omega_0^2$ and $y = m - \Delta^2/2\omega_0^2$ we can write Green's function (D1) as double integral:

$$\begin{aligned} G(\omega, \xi) = {} & \frac{\omega_0^2}{\pi\Delta^2} \int\limits_{-\infty}^{+\infty} dx \int\limits_{-\infty}^{+\infty} dy \exp\left(-\omega_0^2 \frac{x^2 + y^2}{\Delta^2}\right) \times \\ & \times \frac{\omega + \xi}{\omega^2 - \xi^2 - \omega_0^2(x^2 + y^2)}. \end{aligned} \tag{D3}$$

After the obvious transformation to polar coordinates $\rho^2 = x^2 + y^2$ and ϕ, $dxdy \to d\phi\rho d\rho$ we obtain

$$G(\omega,\xi) = \frac{\omega_0^2}{\pi\Delta^2}\int\limits_0^{2\pi} d\phi \int\limits_0^{+\infty} d\rho\rho \exp\left(-\frac{\omega_0^2}{\Delta^2}\rho^2\right) \times \\ \times \frac{\omega+\xi}{\omega^2-\xi^2-\omega_0^2\rho^2}. \quad \text{(D4)}$$

Then introducing $W = \rho\omega_0$ we get

$$G(\omega,\xi) = \int\limits_0^{+\infty} dW \frac{2W}{\Delta^2}\exp\left(-\frac{W^2}{\Delta^2}\right)\frac{\omega+\xi}{\omega^2-\xi^2-W^2}, \quad \text{(D5)}$$

which describes the well known result [6, 7] for the Green's function of an electron moving in a periodic field with a random phase and Rayleigh distributed amplitude.

It can be easily shown that for the case of commensurate fluctuation in the same limit of $\gamma = 0$ and $\omega_0 \ll \Delta$ our double series for the Green's function

$$G(\omega,\xi) = \sum_{n,m=0}^{\infty} P_{\lambda_1}(n)P_{\lambda_2}(m) \times \\ \times \frac{\omega+\xi}{\omega^2-\xi^2-[\omega_0(n-\lambda_1)-\omega_0(m-\lambda_2)]^2}, \quad \text{(D6)}$$

reduces to the simple Gaussian average expression [8]:

$$G(\omega,\xi) = \int\limits_{-\infty}^{+\infty} dW \frac{1}{\sqrt{2\pi}\Delta}\exp\left(-\frac{W^2}{2\Delta^2}\right)\frac{\omega+\xi}{\omega^2-\xi^2-W^2}, \quad \text{(D7)}$$

which corresponds to the case of real order parameter.

APPENDIX E
SOFT PHONON NEAR CDW INSTABILITY AND THE ORIGIN OF DYNAMIC RANDOM FIELD

In the main text the fluctuating order parameter has been treated as a classical Gaussian random field with prescribed temporal correlation function. The purpose of this Appendix is to discuss the microscopic origin of this description and to establish its relation to the conventional electron–phonon Hamiltonian.

Consider the standard electron–phonon interaction,

$$H_{ep} = \sum_{\mathbf{k},\mathbf{q}} g_{\mathbf{q}}\left(b_{\mathbf{q}} + b^{\dagger}_{-\mathbf{q}}\right)c^{\dagger}_{\mathbf{k}+\mathbf{q}}c_{\mathbf{k}}. \quad \text{(E1)}$$

Near a Peierls or charge-density-wave transition the phonon modes with wave vectors close to nesting vector $\mathbf{q} \sim \mathbf{Q}$ soften and at $\mathbf{q} = \mathbf{Q}$ we have $\omega_{\mathbf{Q}} \to 0$. Corresponding Bose occupation numbers become large and

$$n_B(\omega_{\mathbf{Q}}) = \frac{1}{e^{\omega_{\mathbf{Q}}/T}-1} \simeq \frac{T}{\omega_{\mathbf{Q}}}, \quad \text{(E2)}$$

diverges as the transition is approached. The phonon coordinates with $\mathbf{q} \sim \mathbf{Q}$

$$u_{\mathbf{q}} \sim u_{\mathbf{Q}} = \frac{1}{\sqrt{2M\omega_{\mathbf{Q}}}}(b_{\mathbf{Q}} + b^{\dagger}_{-\mathbf{Q}}) \quad \text{(E3)}$$

acquire large thermal fluctuations and behave as an effectively classical stochastic variable. The interaction Hamiltonian may then be approximately written as

$$H_{ep} = \sum_{\mathbf{k}} \Delta(t) c^{\dagger}_{\mathbf{k}+\mathbf{Q}}c_{\mathbf{k}} + \text{H.c.}, \quad \text{(E4)}$$

where $\Delta(t) = g_{\mathbf{Q}}u_{\mathbf{Q}}(t)$. This is precisely the phenomenological Hamiltonian employed throughout the present work.

More formally we can consider the usual finite temperature second-order contribution to retarded electron self-energy due to electron–phonon interaction, obtained by the standard analytical continuation from Matsubara frequencies [5]:

$$\Sigma^R(\omega,\mathbf{k}) = \sum_{\mathbf{q}} |g_{\mathbf{q}}|^2 \left\{ \frac{f_{\mathbf{k}+\mathbf{q}} + n_B(\omega_{\mathbf{q}})}{\omega - \xi_{\mathbf{k}+\mathbf{q}} + \omega_{\mathbf{q}} + i\delta} + \right. \\ \left. + \frac{1 - f_{\mathbf{k}+\mathbf{q}} + n_B(\omega_{\mathbf{q}})}{\omega - \xi_{\mathbf{k}+\mathbf{q}} - \omega_{\mathbf{q}} + i\delta}\right\}, \quad \text{(E5)}$$

where $f_{\mathbf{k}}$ is Fermi function. Now $f_{\mathbf{k}} \sim (1 - f_{\mathbf{k}}) \sim 1$, so that in case of $T \gg \omega_{\mathbf{q}}$ and $n_B(\omega_{\mathbf{q}}) \sim T/\omega_{\mathbf{q}}$ we can rewrite (E5) as

$$\Sigma^R(\omega,\mathbf{k}) = \sum_{\mathbf{q}} |g_{\mathbf{q}}|^2 \frac{T}{\omega_{\mathbf{q}}} \left\{ \frac{1}{\omega - \xi_{\mathbf{k}+\mathbf{q}} + \omega_{\mathbf{q}} + i\delta} + \right. \\ \left. + \frac{1}{\omega - \xi_{\mathbf{k}+\mathbf{q}} - \omega_{\mathbf{q}} + i\delta}\right\}. \quad \text{(E6)}$$

For soft-mode spectrum near Peierls transition we can write

$$\omega_{\mathbf{q}} = \omega_0 + c^2(\mathbf{q}-\mathbf{Q})^2, \quad \text{(E7)}$$

so that approximately we have

$$\Sigma^R(\omega,\mathbf{k}) \approx \sum_{\mathbf{q}} |g_{\mathbf{q}}|^2 \frac{T}{\omega_0 + c^2(\mathbf{q}-\mathbf{Q})^2} \times \\ \times \left\{ \frac{1}{\omega+\xi+\omega_0+i\delta} + \frac{1}{\omega+\xi-\omega_0+i\delta}\right\} = \\ = \frac{1}{2}\Delta^2 \left\{ \frac{1}{\omega+\xi+\omega_0+i\delta} + \frac{1}{\omega+\xi-\omega_0+i\delta}\right\}, \quad \text{(E8)}$$

where we used nesting condition $\xi_{\mathbf{k}} = -\xi_{\mathbf{k}-\mathbf{Q}} = \xi$ and introduced the effective amplitude as

$$\Delta^2 = \sum_{\mathbf{q}} |g_{\mathbf{q}}|^2 \frac{2T}{\omega_0 + c^2(\mathbf{q}-\mathbf{Q})^2}. \qquad \text{(E9)}$$

We see that the soft-mode at the Peierls transition acts as the classical dynamic random field. The same type of behavior is typical for any kind of soft-mode transition. Damping effects naturally lead to finite correlation time of these fluctuations.

Near a soft-mode (Peierls/CDW) transition this mode is usually overdamped as $\gamma \gtrsim \omega_Q$. Resolved dynamic sidebands discussed in the main part of the text require $\omega_0 \gg \Gamma_{\text{eff}}$, i. e., $\omega_0^3 \gg \gamma\Delta^2$, that is an underdamped mode whose frequency exceeds $(\gamma\Delta^2)^{1/3}$. Whether these criteria are satisfied in real materials depends on the values of these parameters in concrete systems.

REFERENCES

1. G. Grüner, *Density Waves in Solids*, Addison-Wesley, Reading, MA (1994).

2. T. Timusk and B. Statt, *The Pseudogap in High-Temperature Superconductors*, Rep. Prog. Phys. **62**, 61 (1999).

3. M. V. Sadovskii, *Pseudogap in High-Temperature Superconductors*, Phys. Usp. **44**, 515 (2001) [Usp. Fiz. Nauk **171**, 539 (2001)].

4. M. V. Sadovskii, *Models of the Pseudogap State in High-Temperature Superconductors*, in *Strings, Branes, Lattices, Networks, Pseudogaps, Dust*, Scientific World, Moscow (2007); arXiv:cond-mat/0408489.

5. M. V. Sadovskii, *Diagrammatics*, 2nd ed., World Scientific, Singapore (2019).

6. M. V. Sadovskii, *A Model of a Disordered System (A Contribution to the Theory of "Liquid Semiconductors")*, Sov. Phys. JETP **39**, 845 (1974) [Zh. Eksp. Teor. Fiz. **66**, 1720 (1974)].

7. M. V. Sadovskii, *Quasi-One-Dimensional Systems Undergoing a Peierls Transition*, Sov. Phys. Solid State **16**, 1632 (1974) [Fiz. Tverd. Tela **16**, 2504 (1974)].

8. W. Wonneberger and R. Lautenschlager, *Theory of Infrared Absorption of Linear Conductors*, J. Phys. C: Solid State Phys. **9**, 2865 (1976).

9. M. V. Sadovskii, *Exact Solution for the Density of Electronic States in a Model of a Disordered System*, Sov. Phys. JETP **50**, 989 (1979) [Zh. Eksp. Teor. Fiz. **77**, 2070 (1979)].

10. M. V. Sadovskii and A. A. Timofeev, *The Two-Particle Green Function in a Model of a One-Dimensional Disordered System: An Exact Solution?* J. Moscow Phys. Soc. **1**, 391 (1991).

11. J. Schmalian, D. Pines, and B. Stojković, *Weak Pseudogap Behavior in the Underdoped Cuprate Superconductors*, Phys. Rev. Lett. **80**, 3839 (1998).

12. J. Schmalian, D. Pines, and B. Stojković, *Microscopic Theory of Weak Pseudogap Behavior in the Underdoped Cuprate Superconductors: General Theory and Quasiparticle Properties*, Phys. Rev. B **60**, 667 (1999).

13. E. Z. Kuchinskii and M. V. Sadovskii, *Models of the Pseudogap State of Two-Dimensional Systems*, JETP **88**, 968 (1999) [Zh. Eksp. Teor. Fiz. **115**, 1765 (1999)].

14. M. V. Sadovskii, I. A. Nekrasov, E. Z. Kuchinskii, Th. Pruschke, and V. I. Anisimov, *Pseudogaps in Strongly Correlated Metals: A Generalized Dynamical Mean-Field Theory Approach*, Phys. Rev. B **72**, 155105 (2005).

15. E. Z. Kuchinskii, I. A. Nekrasov, and M. V. Sadovskii, *Pseudogaps in Strongly Correlated Metals: Optical Conductivity within the Generalized Dynamical Mean-Field Theory Approach*, Phys. Rev. B **75**, 115102 (2007).

16. E. Z. Kuchinskii, I. A. Nekrasov, and M. V. Sadovskii, *Generalized Dynamical Mean-Field Theory in the Physics of Strongly Correlated Systems*, Phys. Usp. **55**, 325 (2012) [Usp. Fiz. Nauk **182**, 345 (2012)].

17. M. Ye, Z. Wang, R. M. Fernandes, and A. V. Chubukov, *Location and Thermal Evolution of the Pseudogap due to Spin Fluctuations*, Phys. Rev. B **108**, 115156 (2023).

18. M. Ye and A. V. Chubukov, *Crucial Role of Thermal Fluctuations and Vertex Corrections for the Magnetic Pseudogap*, Phys. Rev. B **108**, L081118 (2023).

19. E. Z. Kuchinskii and M. V. Sadovskii, *Generalized Dynamical Keldysh Model*, JETP **166**, 42 (2024) [Zh. Eksp. Teor. Fiz. **166**, 45 (2024)]; arXiv:2401.08118.

20. M. N. Kiselev and K. Kikoin, *Scalar and Vector Keldysh Models in the Time Domain*, JETP Lett. **89**, 114 (2009) [Pis'ma Zh. Eksp. Teor. Fiz. **89**, 133 (2009)].

21. D. V. Efremov and M. N. Kiselev, *Seven Études on Dynamical Keldysh Model*, SciPost Phys. Lect. Notes **65** (2022); arXiv:2206.06609.

22. Y. Nambu, *Quasi-Particles and Gauge Invariance in the Theory of Superconductivity*, Phys. Rev. **117**, 648 (1960).

23. V. G. Vaks, A. I. Larkin, and S. A. Pikin, *Spin Waves and Correlation Functions in a Ferromagnet*, Sov. Phys. JETP **26**, 647 (1968) [Zh. Eksp. Teor. Fiz. **53**, 1089 (1967)].

24. Yu. A. Izyumov, F. A. Kassan-Ogly, and Yu. N. Skryabin, *Diagram Technique for Spin-Operators and Its Applications to Some Problems of Ferromagnetism*, J. Phys. Colloq. **32**, C1-86 (1971).

25. Yu. A. Izyumov and Yu. N. Skryabin, *Statistical Mechanics of Magnetically Ordered Systems*, Consultants Bureau, New York (1988).

26. V. G. Bar'yakhtar, V. N. Krivoruchko, and D. A. Yablonskii, *Spin Green Functions and the Problem of Summation over Physical States*, Sov. Phys. JETP **58**, 351 (1983) [Zh. Eksp. Teor. Fiz. **85**, 601 (1983)].

27. V. I. Belinicher and V. S. L'vov, *Spin Diagram Technique for Nonequilibrium Processes in the Theory of Magnetism*, Sov. Phys. JETP **59**, 564 (1984) [Zh. Eksp. Teor. Fiz. **86**, 967 (1984)].

28. W. Magnus, *On the Exponential Solution of Differential Equations for a Linear Operator*, Commun. Pure Appl. Math. **7**, 649 (1954).

29. R. Kubo, *Generalized Cumulant Expansion Method*, J. Phys. Soc. Jpn. **17**, 1100 (1962).

30. R. Kubo, *Note on the Stochastic Theory of Resonance Absorption*, J. Phys. Soc. Jpn. **9**, 935 (1954).

31. L. P. Gor'kov, *On the Energy Spectrum of Superconductors*, Sov. Phys. JETP **7**, 505 (1958) [Zh. Eksp. Teor. Fiz. **34**, 735 (1958)].

32. T. Moriya, *Spin Fluctuations in Itinerant Electron Magnetism*, Springer, Berlin, Heidelberg (1985).

33. B. I. Halperin and T. M. Rice, *The Excitonic State at the Semiconductor-Semimetal Transition*, in *Solid State Physics*, ed. by F. Seitz, D. Turnbull, and H. Ehrenreich, Academic Press, New York (1968), Vol. 21, p. 115.

34. E. Z. Kuchinskii, I. A. Nekrasov, and M. V. Sadovskii, *Electronic Structure of Two-Dimensional Hexagonal Diselenides: Charge Density Waves and Pseudogap Behavior*, JETP **114**, 671 (2012) [Zh. Eksp. Teor. Fiz. **141**, 767 (2012)].

35. A. Damascelli, Z. Hussain, and Z.-X. Shen, *Angle-Resolved Photoemission Studies of the Cuprate Superconductors*, Rev. Mod. Phys. **75**, 473 (2003).